

Experimentally Induced Visual Projections to the Auditory Thalamus in Ferrets: Evidence for a W Cell Pathway

ANNA W. ROE, PRESTON E. GARRAGHTY, MANUEL ESGUERRA,
AND MRIGANKA SUR

Department of Brain and Cognitive Sciences, Massachusetts Institute of Technology,
Cambridge, Massachusetts 02139

ABSTRACT

We have previously reported that following specific neonatal brain lesions in ferrets, a retinal projection is induced into the auditory thalamus (Sur et al., *Science* 242:1437, '88). In these "rewired" ferrets, a novel visual pathway is established through auditory thalamus [the medial geniculate nucleus (MGN)] and primary auditory cortex (A1); cells in both MGN and A1 are visually responsive and exhibit properties similar to those of visual cells in the normal visual pathway.

In this paper, we use three approaches—physiological, anatomical, and developmental—to examine which of the retinal ganglion cells project to the MGN in these rewired ferrets. We find that: 1) physiological response properties of postsynaptic visual cells in the MGN are W-like; 2) retinal ganglion cells back-filled from the MGN are small and similar to soma sizes of subsets of the normal retinal W cell population; and 3) subpopulations of these small cells can be preferentially rerouted to the MGN in response to different surgical manipulations at birth, consistent with differential W cell projection patterns in normal animals. These data suggest that retinal W cells come to project to the MGN in rewired animals. These findings not only provide a basis on which to interpret functional properties of this novel visual pathway, but also provide important information about the developmental capabilities of specific retinal ganglion cell classes and the regulation of their projections by target structures in the brain during development. © 1993 Wiley-Liss, Inc.

Key words: X, Y, retinal ganglion cell, development, plasticity

In ferrets, specific neonatal lesions result in the redirection of some retinal ganglion cells into nonvisual thalamic targets, specifically, the auditory thalamic relay nucleus, the medial geniculate nucleus (MGN) (Sur et al., '88). This "rewiring" of retinal input produces a novel visual pathway to primary auditory cortex via the MGN (Sur et al., '88). Such a preparation provides a novel approach to studying the relative contributions of afferent and target to the generation of thalamic and cortical visual receptive field properties. Crucial to this approach is the identification of the specific retinal cell classes from which this pathway originates.

The normal ferret retina contains three classes of ganglion cell (termed, as in cats, X, Y, and W), each with distinct morphologies and physiologies (Henderson, '85; Vitek et al., '85; Roe et al., '89). The X and Y cell classes are each rather homogeneous in structure and function: X cells have medium-sized somata and small receptive fields, exhibit linear spatial and temporal summation, and project primarily to the lateral geniculate nucleus (LGN); Y cells

have large somata and large receptive fields, respond nonlinearly to spatial and temporal summation, and project primarily to both the LGN and the superior colliculus (SC). In contrast, W cells are much more heterogeneous as a class. They have small to medium sized somata, diverse physiological characteristics (often poor spatial and temporal sensitivities, slow axonal conduction velocities, sluggish responsiveness, and large receptive fields), and diverse patterns of retinofugal projections (including the C laminae of the LGN and the superficial gray of the SC). Indeed, the term "W cells" may encompass several distinct subclasses

Accepted April 1, 1993.

Address reprint requests to Anna W. Roe at her present address, Division of Neuroscience, Baylor College of Medicine, S-603 One Baylor Plaza, Houston, TX 77030.

Preston E. Garraghty's present address is Dept. of Psychology, Program in Neural Science, Indiana University, Bloomington, IN 47405.

Manuel Esguerra's present address is Graduate Dept. of Biochemistry, Brandeis University, Waltham, MA 02254.

of retinal ganglion cells. In addition to anatomical and physiological features, a third potentially useful source of evidence for differentiating retinal ganglion cell classes is their normal patterns and modes of development and their responses to abnormal sensory inputs during development. X and Y axons are known to develop in quite distinct manners both in the normal LGN and in response to alterations of normal visual input during development (for review, see Sur, '88; Garraghty and Sur, '88). While not much is known about the developmental capabilities of retinal W cells, it is established that many small retinal ganglion cells (W cells?) are among the last to be born in the retina (Walsh et al., '83). Thus it is possible that these cells would be the most likely to project to a novel target (such as the MGN) after postnatal manipulations. If so, their normally diverse termination patterns could be reflected in the selective innervation of the MGN by different subtypes of W cells following lesions of the LGN or the SC. That is, the response of the novel retino-MGN projection to selective lesions of normal targets could provide additional clues to the identity of the projection. In this paper, we use these three approaches—physiological, anatomical, and developmental characterization—to examine the possibility that W retinal ganglion cells project to the MGN of rewired ferrets.

MATERIALS AND METHODS

Neonatal surgery to produce retinal innervation of MGN

Procedures are similar to those described previously (Sur et al., '88; Pallas et al., '90). Briefly, timed pregnant pigmented ferret jills were bred in our colony or purchased from a commercial supplier (Marshall Farms). Within 24 hours of parturition, ferret kits were removed and anesthetized by deep hypothermia. All surgery was performed under sterile conditions. A 1.0 cm midline incision was made in the scalp, and the skull was exposed. After a small piece of overlying skull was removed, the SC was ablated by heat cautery. To induce massive retrograde degeneration of the LGN, large regions of visual cortex (including areas 17, 18, and 19) were lesioned by cauterizing through the skull. Fibers running in the brachium of the inferior colliculus were transected at mid-SC level, thereby denervating the MGN. All lesions were made unilaterally. On completion of surgery, the skin was sutured and the kit revived under a heat lamp. A single dose of antibiotics (0.01 ml amoxicillin, 100 mg/ml) was given subcutaneously, and antibacterial ointment was applied to the wound. The kit was then returned to the mother for rearing. These procedures, which combine severe reduction of the two major retinal targets with creation of alternative target space in the MGN, lead to induction of developing retinofugal afferents to the MGN (Sur et al., '88; cf. Schneider, '73).

Visual physiology in adult ferrets

Surgical preparation. Normal and rewired adult ferrets were prepared for visual physiology by procedures similar to those described previously (Roe et al., '89). Normal ferrets were pigmented Sable ferrets obtained from Marshall Farms. All experimental ferrets used for physiological recordings had received lesions of the visual cortex, SC, and brachium of the inferior colliculus at birth as described above. Animals were anesthetized, paralyzed, and ventilated. Following induction of anesthesia with ketamine hydrochloride (30 mg/kg) and xylazine (2 mg/kg), a can-

nula (24 g) for anesthetic and paralytic delivery was implanted in either the femoral or the jugular vein, and an endotracheotomy was performed. Animals were then placed in a stereotaxic apparatus, paralyzed with a bolus of gallamine triethiodide, and artificially ventilated (rate 30–40/min, volume 25–30 cc) with a 70/30 mixture of nitrous oxide/oxygen. Ferrets received a constant intravenous infusion of a 5% dextrose solution containing ketamine hydrochloride (10 mg/kg/hr) for anesthesia and gallamine triethiodide (3.6 mg/hr/kg) for muscular paralysis. End-tidal CO₂ was maintained at 4.0%, heart rate monitored, and body temperature maintained at 38°C with a heating pad. Supplemental halothane (1%) was supplied during all surgical procedures. The skull and dura over cortex above lateral thalamus were removed. Drops of atropine sulfate and phenylephrine hydrochloride were applied to the eyes to dilate the pupils. Eyes were fitted with zero power contact lens and focused on a tangent screen 114 cm in front of the animal. Optic disks were plotted by reflection onto the tangent screen and used to determine the locations of visual receptive fields. Stimulating electrodes were lowered into the optic chiasm and cemented in place.

Recording and data collection. We used parylene insulated tungsten microelectrodes (2–3 megohm impedances) to record extracellularly from thalamic cells of 14 rewired ferrets and 4 normal ferrets. Initial recording penetrations were made on the basis of stereotaxic coordinates for the LGN in normal ferrets (Zahs and Stryker, '85; see Results). Upon reaching thalamus, unit activity was assessed every 50–100 μm in each penetration for: 1) response to electrical stimulation of the optic chiasm; and 2) response to visual stimulation. In two rewired animals and one normal animal, broad-band auditory stimuli (100 msec square-wave clicks or bursts of white noise) were delivered through earphones. Visually responsive units were plotted and characterized on the tangent screen with a hand-held projection lamp. In addition to receptive field location and size, a number of other response characteristics were also examined. These included the contrast of the center response (on or off), ocular dominance, linearity of spatial summation, orientation-selectivity, direction-selectivity, velocity preference, presence or absence of an inhibitory surround, and strength of center response. Electrolytic lesions (5 μA for 5 seconds) or tracer injections (see below) were made in selected penetrations.

For quantitative determination of orientation and direction preferences, moving bar stimuli, either projected with an optic bench or generated on a Tektronix monitor driven by a Picasso stimulus generator (Innisfree), were swept at different orientations over the receptive field. Spike responses of the cell under study were isolated with a pulse-shape discriminator (Ealing). For each stimulus, 20 cycles were collected and summed by the Unkelscope Program run on an IBM PC 286 computer and poststimulus time (PST) histograms generated on-line. Spike responses were also stored on tape and PST histograms analyzed off-line.

Histology. Following the completion of data collection, the animal was sacrificed with an intravenous or intraperitoneal overdose of pentobarbital (65 mg/kg) and perfused through the heart with saline followed by fixative (1% paraformaldehyde, 2% glutaraldehyde) and 10% and 20% sucrose solutions. The brain was then removed from the cranium and stored in 30% sucrose overnight. After brain sulcal patterns were recorded photographically, frozen sec-

tions were cut at 50 μm and were Nissl-stained. Lesions and recording tracks were located and reconstructed.

Retinal ganglion cells filled retrogradely in rewired and normal ferrets

Thalamic horseradish peroxidase injections. In five rewired ferrets and four normal ferrets, injections of tracers were made in thalamus. Placement of tracer injections were made either under stereotaxic guidance or in combination with physiological recordings (see above). For large thalamic injections, up to 1 μl of 20% horseradish peroxidase (HRP) was injected with a Hamilton syringe. For more restricted injections, 10% HRP was iontophoresed through a glass micropipette (impedance 10–30 megohms) for 15–30 minutes (0.6–1.0 μA at 0.5 sec on, 0.5 sec off). This produced HRP deposits 0.25–1.0 mm in diameter.

Depending on the type of experiment being conducted, transport time ranged from 12 hours to 3–4 days. Animals were then given an overdose of pentobarbital (65 mg/kg) and perfused through the heart with saline followed by fixative (1% paraformaldehyde and 2% glutaraldehyde in 0.1 M phosphate buffer), and then 10% and 20% sucrose solutions. Brains and retinae were removed and stored overnight. In brains in which HRP injections had been made, alternate brain sections (cut at 100 μm) were processed for HRP visualization with diaminobenzidine intensified with cobalt chloride. HRP back-filled retinae were processed with O'dianisidine (DeOlmos, '77) and flat-mounted.

Data analysis. Location and extent of each thalamic injection was determined and soma sizes of back-filled retinal ganglion cells measured. To compare retinal ganglion soma size populations from different retinae, in all but two cases, measurements were taken from each retina contralateral to the injected hemisphere at a region superior to area centralis corresponding approximately to the 1,500 cells/ mm^2 isodensity contour of Henderson ('85). In the other two cases, retinal ganglion cells were back-filled from the SC and only the retina nasal to the optic disk was labelled. In these cases, measurements were taken from the 1,500 cells/ mm^2 isodensity contour approximately midway between the optic disk and the nasal retinal border. At these locations in each retina, back-filled retinal ganglion somata were drawn with a camera lucida attachment at a final magnification of $\times 670$; all back-filled cells within each single field of view were drawn and as many adjacent fields of view were drawn as required to reach a number of at least 100 cells/retina. Soma areas were subsequently measured with a SummaSketch digitizing pad run by SigmaScan software on an IBM PC 286. Distributions, means, and variances were calculated and the nonparametric Mann-Whitney U test used for comparison of soma size measurements.

Selective redirection of retinal ganglion cell subpopulations

Surgery. We reasoned that considerable insight could be gained into the nature and source of retinal inputs to the MGN by examining their response to changes in target availability. By using various combinations of each of three neonatal lesions, we thus varied the amount and type of available target space for developing retinal afferents (the major targets being the LGN and SC), and subsequently examined the resulting retinal innervation in the MGN. Lesions that reduced normal retinal target zones included:

1) ablation of visual cortex (VCX) (which results in massive retrograde degeneration of the LGN); and 2) direct ablation of the SC. The third lesion, transection of the brachium of the inferior colliculus (BC), denervated the MGN and increased alternative target space, albeit in an aberrant zone. We performed the following seven combinations of lesions (see neonatal surgery) in neonatal ferrets and examined the distribution of the resulting retino-MGN projection at adulthood:

1. VCX + SC + BC (n = 2)
2. VCX + BC (n = 3)
3. SC + BC (n = 3)
4. VCX + SC (n = 1)
5. VCX (n = 2)
6. SC (n = 2)
7. BC (n = 1)

Two additional ferrets (one VCX + BC, one SC + BC) were used for thalamic injection and retinal backfill experiments following procedures described above, for comparison with the five rewired (VCX + SC + BC) and four normal animals.

Eye injections, histology, and autoradiography. After these operated ferrets were raised to adulthood, 20 μl of 20% HRP and 1% wheat germ agglutinin-conjugated (WGA)-HRP was injected with a Hamilton syringe into the eye contralateral to the operated hemisphere. Following a 3–5 day survival, the animal was given an overdose of pentobarbital (65 mg/kg) and perfused through the heart with fixative (1% paraformaldehyde/2% glutaraldehyde) and 10% and 20% sucrose in phosphate buffers, and subsequently stored in 30% sucrose in phosphate buffer overnight. The brain was then sectioned and processed with tetra methyl benzidine (TMB) histochemistry (Mesulam, '78). Following mounting, clearing, and coverslipping, the sections were then examined for HRP reaction product.

In two animals, a second tracer, ^{35}S -methionine, was additionally injected into the eye ipsilateral to the lesioned hemisphere. In these cases, several series of the thalamic sections were dipped in NTB-2 (Kodak) photographic emulsion, dried, and stored in the dark. Periodically (between 2 weeks and 2 months), series of exposed sections were photographically developed, cleared, and coverslipped. One series of sections from each animal was chosen for subsequent analysis.

Data analysis. Retinal terminal label in the thalamus was mapped and quantified in each case. In each animal that had received an eye injection, the LGN, MGN, and regions of retinal label were drawn by camera lucida at a magnification of $58\times$. The areas of the LGN, the MGN, and the zones of labelled retinofugal axons in each section were measured with a SummaSketch digitizing pad run by SigmaScan software on an IBM PC 286. The volume of each zone was then determined by multiplying the area of the zone by the inter-section distance. The size of retinal projection to the MGN was then calculated as a percentage of the MGN volume in each animal.

RESULTS

We present three types of data to examine the source of retinal projections to the MGN in rewired animals. These include: 1) physiological characterization of the postsynaptic visual cells in the MGN; 2) morphological characteriza-

TABLE 1. Number of Units Recorded in the Medial Geniculate Nucleus (MGN)¹

	MGN
Total	238 (100)
Electrically driven	226 (95)
Visually driven	131 (55)
Visually and electrically driven	123 (52)
Receptive field location determined	105 (44)
Responsivity rated	46 (19)
Receptive field size determined	40 (17)
Ocular dominance determined	73 (31)
Quantitatively characterized for	
Orientation	10 (9)
Direction	21 (4)
Driven by auditory stimuli	4 (15) ²
Driven by auditory and visual stimuli	3 (11) ²

¹Percent is in parentheses.

²Calculated from a total of 27 units tested with auditory stimulation in two experiments.

tion (chiefly soma size measurements) of retinal ganglion cells projecting to the MGN; and 3) selective redirection of retinal ganglion cell subpopulations.

Physiological properties of visual cells in the MGN

To identify the functional class(es) of retinal ganglion cell giving rise to the aberrant retino-MGN projection, one would ideally record from retinal ganglion cells back-fired from the MGN and characterize the features of these cells. Given the substantial technical difficulty of such an experiment, however, an alternative approach is to record from retinal afferent fibers projecting to the MGN or from MGN cells postsynaptic to the retinal afferent terminations. In view of the similarity in response characteristics of retinal and geniculate X, Y, and W cells (Stanford, '87a; Sur and Sherman, '82; for review, see Sherman and Spear, '82), we find it reasonable to expect that the visual response characteristics of MGN cells will be indicative of their presynaptic retinal input. The validity of this interpretation will be further examined in the discussion.

We examined the responses of thalamic cells in 11 rewired (VCX + SC + BC) ferrets to electrical stimulation of the optic chiasm, to visual stimulation, and, in two experiments, to auditory stimulation. The placements of our initial penetrations in each experiment were based on stereotaxic coordinates of the normal LGN. In rewired ferrets the LGN tended to be shifted rostrally and medially with respect to the location of the LGN in normal animals. Along the depth of each penetration, thalamic recordings were usually preceded by characteristic hippocampal activity (highly active cells with large amplitude spikes) followed by silence as the electrode advanced through the lateral ventricle. In any penetration in which both LGN and MGN cells were recorded, the transition between LGN and MGN was quite evident, often marked by an immediate decrease in background activity and briskness of response to visual stimulation, and sudden shift in visual topography (cf. Roe, '91; Roe et al., '91). We report on units histologically determined to be in all three major divisions of the MGN—the ventral (MG_v), medial (MG_m), and dorsal (MG_d) divisions (Morest, '65).

Of a total of 238 units recorded in the MGN, almost all (95%) were electrically driven from the chiasm and approximately half (55%) were visually driven (Table 1). Auditory responsiveness was observed in 7 of 27 units tested.

Responses to electrical stimulation: latency of spike responses. Two hundred and twenty-six MGN units (recorded from 14 rewired ferrets) were driven by electrical

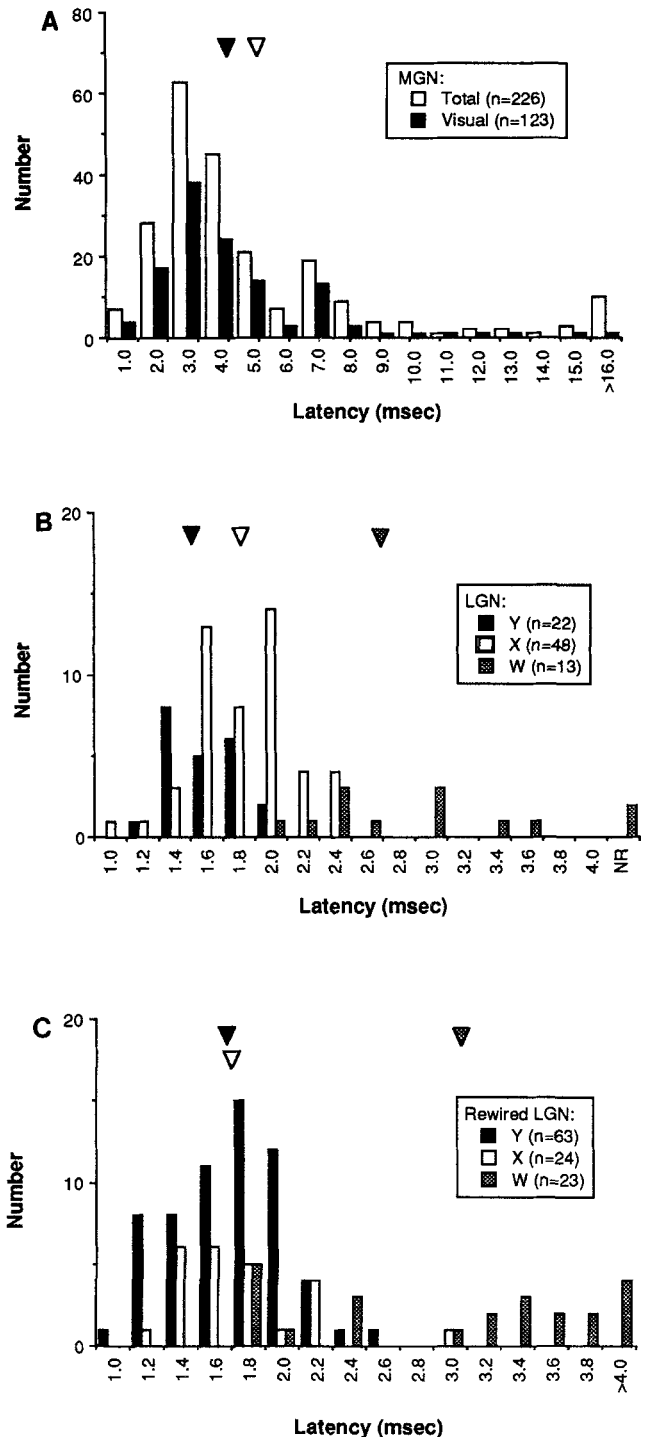


Fig. 1. Latencies to electrical stimulation of the optic chiasm of (A) medial geniculate nucleus (MGN) cells in rewired ferrets, (B) lateral geniculate nucleus (LGN) cells of normal ferrets, and (C) LGN cells in rewired ferrets. Inverted triangles denote mean values.

stimulation of the optic chiasm (Table 1, Fig. 1A). Cellular responses were usually bimodal (negative-positive) and sometimes trimodal (negative-positive-negative) in waveform. Jitter in latencies (defined as the time from the optic chiasm shock to the first elicited spike) for any single unit

usually fell within a 1.0 msec range, and synaptic failure was elicited at high rates of stimulation (10–100 shocks/sec). For each unit, the mode of the latencies elicited by multiple chiasm shocks was taken as the cell's spike latency to optic chiasm stimulation. Retinal afferents (recognized by monophasic spike responses that exhibit no synaptic failure even at high stimulation rates and no jitter in latency), recorded commonly in the LGN (Roe et al., '89), were recorded rarely in the MGN. This is likely due to the small size of the afferent axons (Pallas et al., '90), particularly in relation to electrode tip size, and the relative sparseness of the projection (see below). Almost all units (94%) driven visually were responsive to electrical stimulation of the optic chiasm.

Latencies of MGN cells were longer than those of X or Y cells in the normal LGN. Normal LGN X cell latencies ranged from 1.1 to 2.5 msec ($n = 48$, mean = 1.9 msec), while those of LGN Y cells ranged from 1.2 to 2.1 msec ($n = 22$, mean = 1.6 msec). Consistent with observations from cats (e.g., Hoffmann, '73; Berson, '87), the latencies of normal LGN W cells (range 2.1–3.7 msec, $n = 13$, mean = 2.8 msec) were longer than most X and Y cell latencies; two normal LGN W cells were not responsive (NR) to chiasm shocks (Fig. 1B).

Latencies of MGN cells ($n = 226$) spanned quite a large range (1.5–35.0 msec, mean = 5.6 msec), the majority of which (80%) fell between 2.0 and 7.0 msec (Fig. 1A). The latencies of the visually responsive subpopulation ($n = 123$, mean = 4.8 msec) exhibited a very similar distribution (Fig. 1A). These latencies were significantly longer than those of normal LGN X (Mann-Whitney U test, $P < 0.0001$) or Y ($P < 0.0001$) cells; 85% of the MGN latencies were longer than any recorded for LGN X and Y cells. Another 13% of the MGN latencies (those falling in the 2 msec range) overlapped with the lower range of LGN W cell latencies and the upper range of LGN X cell latencies; there was virtually no overlap between MGN latencies and LGN Y cell latencies.

The overlap in the latency distribution with LGN W cell latencies was considerable: 61% of the MGN latencies fell into the 2.0–4.0 msec range. A second small peak in the MGN latency distribution occurred at 7.0–8.0 msec, perhaps indicating the presence of a second, more slowly conducting population reaching the MGN. In the normal cat retina, two subpopulations of W cells have slow and very slow axonal conduction velocities, respectively (Hoffmann, '73; Cleland and Levick, '74a; Berson, '87; Stanford, '87a). The large range of these latencies recorded in the MGN (up to > 16.0 msec) may also be indicative of heterogeneity in W cell input, as is characteristic of the normal retinal W cell population (e.g., Cleland and Levick, '74b).

To address the possibility that, in the rewired ferrets, retinal axons of all cell classes may have longer optic chiasm latencies, we recorded latencies of LGN cells to optic chiasm stimulation as well (Fig. 1C). There was a prominent reduction (from 62% to 22%) in the percentage of X cells recorded in rewired ferret LGN (Sur et al., '87; cf. Tong and Spear, '82). However, the latency distributions of Y (range 1.1–2.7 msec, $n = 61$, mean = 1.8 msec), X (range 1.2–3.0, $n = 24$, mean = 1.8 msec), and W (range 1.8–5.8 msec, $n = 23$, mean = 3.1 msec) cells were not significantly different from their normal LGN counterparts (Mann-Whitney U test: Y, $P > 0.13$; X, $P > 0.18$; W, $P > 0.30$). These data indicate that, at least for retinal afferents projecting to the

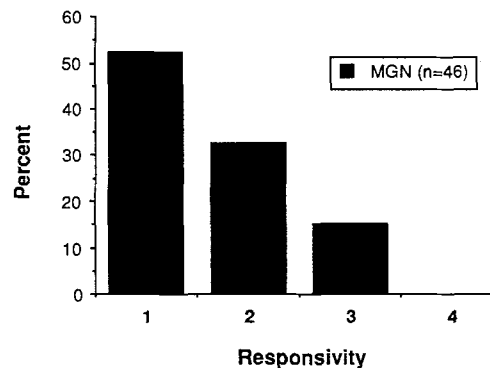


Fig. 2. Responsivity ratings for visual (MGN) cells ($n = 46$) from three rewired ferrets. 1 indicates low responsivity; 4 indicates responsivity comparable to that of normal X and Y LGN cells.

LGN, conduction latencies are not affected in some nonspecific fashion by the neonatal lesions.

Responses to visual stimulation

Response characteristics. Response characteristics of visual MGN cells were reminiscent of those previously described for retinal and LGN W cells (Cleland et al., '71; Sur and Sherman, '82), both in terms of response quality and in terms of diversity. In general, responsiveness of cells in the MGN to visual stimulation was poor in comparison to those of X and Y LGN cells in normal ferrets. Whereas normal LGN X and Y cells responded briskly and consistently to flashing or moving bars and spots, these same visual stimuli produced much weaker, more labile, "sluggish" responses in visual MGN cells. Such sluggishness of response was also found in some W cells recorded in the LGN. We qualitatively rated the responsiveness of visual MGN cells in three experiments. Each visual unit recorded was given a responsivity rating ranging from 1 to 4, with 1 indicating low responsivity and 4 a responsivity comparable to those of normal LGN X and Y cells. This responsivity index reflected both strength and consistency of response. Of 46 visual cells rated in this manner (35% of all visual cells recorded), over half were given a rating of 1, and none were rated as 4 (Fig. 2). A further reflection of poor responsiveness is the significant proportion of units (Table 1) that were driven by chiasm stimulation but were visually unresponsive (cf. Wilson et al., '76). Thus, reliable determination of visual receptive field properties in the MGN required careful and time-consuming, repetitive, visual stimulation.

MGN cells turned out to be diverse in their response features. Some MGN cells exhibited a moderate level of spontaneous activity, which was modulated by visual stimuli (Figs. 3A,B, 4A). In contrast, a few cells exhibited virtually no background activity and responded to visual stimuli with only a few spikes or even a single spike. Most MGN cells responded to either onset ($n = 30$, Fig. 3A) or offset ($n = 23$, Fig. 3B) of light stimuli, and a few ($n = 6$) responded to both stimulus onset and offset. (In comparison, the few on/off cells recorded in the LGN of normal animals were of the W cell class; all X and Y cells were either on-center or off-center.) MGN cells preferred slowly flashing spots in their receptive field, and often "fatigued" with prolonged stimulus presentation. For some cells, only if the frequency of stimulation was extremely low (e.g., less than 0.5 Hz) could responses be consistently elicited. Ten of 131

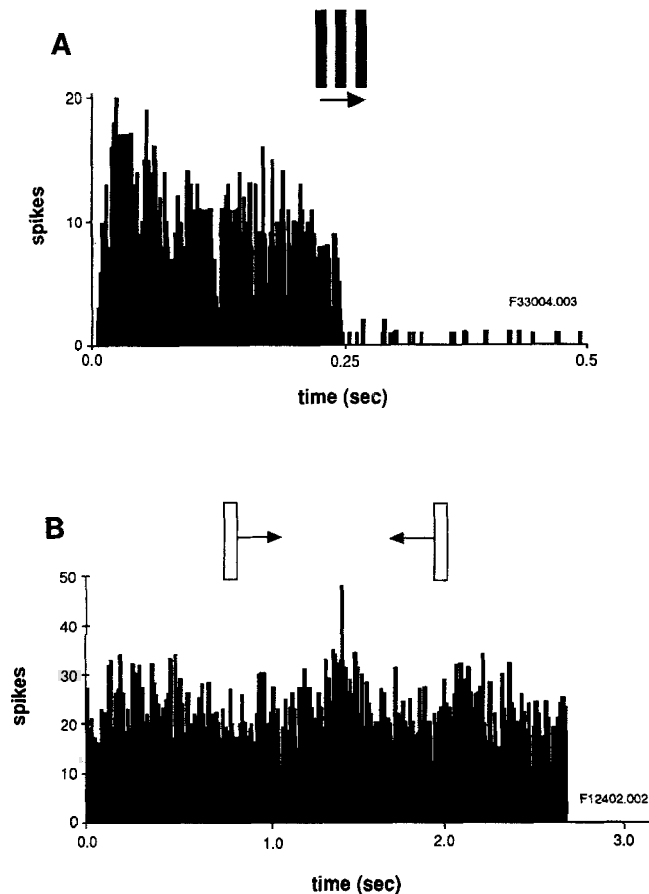


Fig. 3. On and off cells in the MGN. **A:** On-center cell responds to a square-wave grating (0.25 cyc/deg) drifting at 2 Hz. Sum of 20 cycles. This cell responds in each cycle to a light bar moving through its receptive field and is silent when the dark bar passes through. **B:** Off-center cell responding to a moving bar. The activity level of this off-center cell is slightly depressed by a light bar passing over its receptive field. Bar size, 1.8×11.3 degrees; bar velocity, 8.7 degrees/sec. Sum of 30 cycles.

cells responded only to very strong stimuli, such as full field flashes. All units were monocularly driven, with a predominant contralateral bias (contralateral, $n = 69$; ipsilateral, $n = 4$).

Visually driven MGN cells were not orientation selective. MGN cells exhibited similar responses to bars flashed at different orientations within their receptive fields and to bars swept at different orientations across their receptive fields. We quantified orientation tuning for a small population of MGN cells ($n = 10$). We defined an orientation tuning index as: $1 - (\text{Orthogonal Response/Peak Response})$ (cf. Felleman and Van Essen, '87). A cell whose response in the best orientation is twice that in the orthogonal orientation would have an orientation selectivity index of 0.5; one whose best response is 1.5 times that in the orthogonal orientation would have an index of 0.33. As a rule of thumb, we consider those units with indices below 0.3 to be unoriented, those with indices from 0.3 to 0.5 to be broadly oriented, and those with indices above 0.5 to be sharply oriented. All MGN cells had orientation indices below 0.3 (range 0.0–0.29, mean = 0.11). Figure 4A illustrates an MGN cell from our sample with the highest

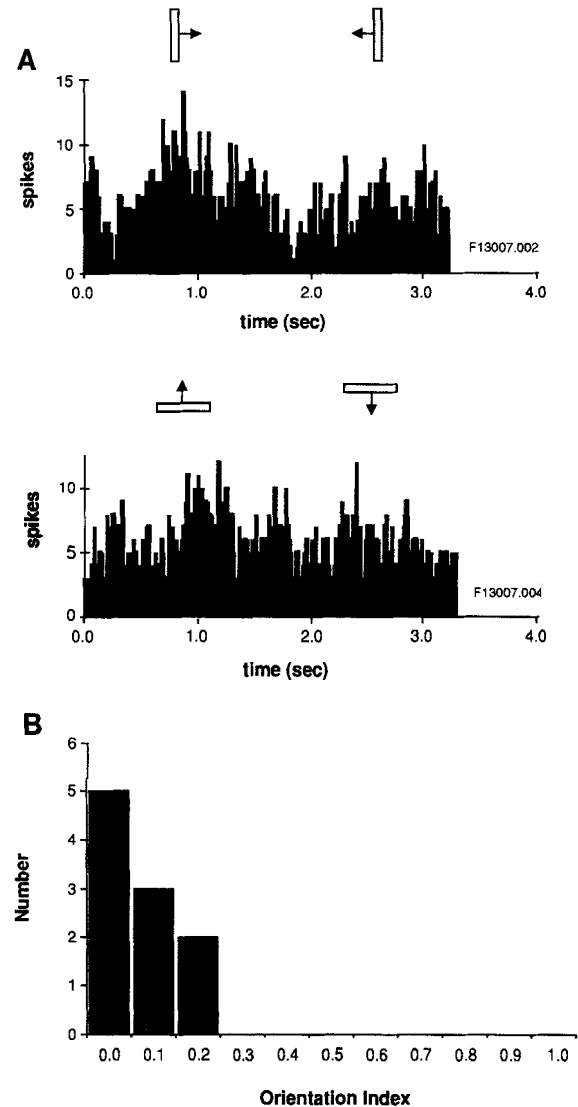


Fig. 4. MGN cells are not selective for orientation. **A:** Poststimulus time histograms illustrate the response of an MGN cell to a moving vertically oriented bar of light (upper) and to a moving horizontally oriented bar of light (lower). This cell had the highest orientation index (0.29) of the ten MGN cells studied in this fashion. Its directionality index is 0.24. Bar size 2×25 degrees, moving at 15 degrees/sec. Sum of 20 cycles. **B:** Distribution of orientation indices of MGN cells ($n = 10$, mean = 0.11, range 0.0–0.29). See text for details.

orientation tuning index (0.29). Figure 4B displays the distribution of all orientation tuning indices obtained in our sample. [This distribution contrasts sharply with the orientation tuning indices obtained for visual cells in primary auditory cortex of rewired ferrets (range 0.0–0.79, mean = 0.41; see Roe et al., '92, Fig. 8A).]

Some MGN cells preferred moving stimuli to flashing stimuli. Slowly moving ($< 5^\circ/\text{sec}$) stimuli were most effective in eliciting responses from most cells. A few cells responded well to large rapidly moving, or to rapidly jiggling, bars or spots. Directional selectivity was also seen. Figure 5A illustrates an MGN cell excited by a bar of light sweeping in one direction but inhibited by the bar sweeping in the opposite direction. We quantified direction selectivity

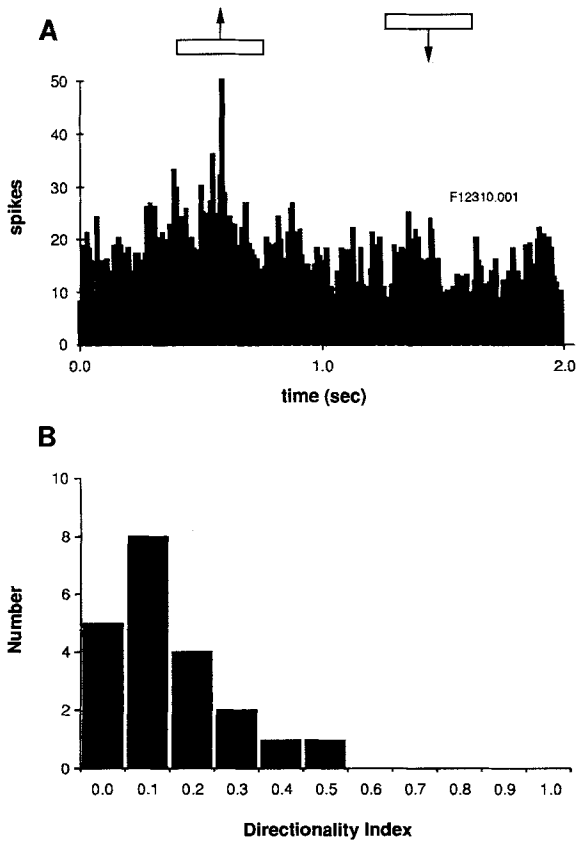


Fig. 5. Directional selectivity of MGN cells. **A:** Poststimulus time histogram illustrates a directionally selective MGN cell. Directionality index 0.5. Stimulus is 2×8 degrees bar moving at 6 degrees/sec. Sum of 20 cycles. **B:** Directionality indices of MGN cells ($n = 21$, range 0.02–0.50, mean = 0.18). See text for details.

using a directionality index defined as: $1 - (\text{Non-Preferred} / \text{Preferred Response})$. The directionality indices of 21 MGN cells that were quantitatively studied for this purpose ranged from 0.02 to 0.50 (mean = 0.18). Of these, 17 MGN cells were nondirectional (index < 0.3), 4 were moderately directional (index 0.3–0.5), and none highly directional (index > 0.5) (Fig. 5B). [These indices are again significantly different from those of visual cells in A1 of rewired ferrets: range 0.0–0.79, mean = 0.45 (see Roe et al., '92, Fig. 9).]

Receptive field size. Receptive fields were circular or slightly elongated and exhibited either weak or absent inhibitory surrounds (not unlike many normal LGN cells; cf. Price and Morgan, '87; Roe et al., '89). Receptive field sizes of MGN cells were, in general, quite large. Of the 105 MGN cells whose receptive field locations were determined, 38% ($n = 40$) were sufficiently responsive to allow confident characterization of receptive field size. Receptive field sizes (defined as the average diameter of the long and the short axis of the receptive field) of MGN cells ranged from 1° to over 16° in diameter and were significantly larger than those of normal LGN cells (Mann-Whitney U, $P < 0.0001$, Fig. 6A). These differences in receptive field size are not eccentricity related (Fig. 6B): when eccentricity-matched LGN and MGN cell populations (eccentricity $< 30^\circ$) are compared, receptive field sizes of MGN cells are still larger

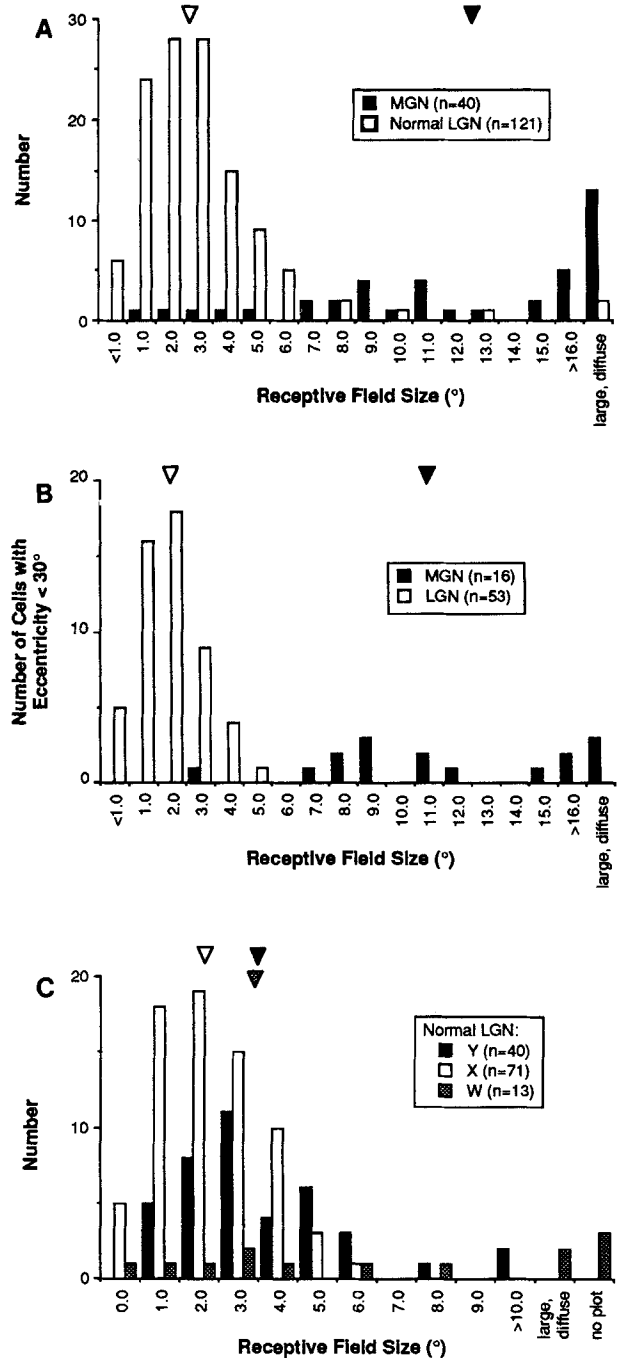


Fig. 6. Receptive field sizes (in degrees, calculated as the average diameter of the long and the short axes of the receptive field) of (A) MGN ($n = 40$, mean = 13.1 degrees) and normal LGN (light bars, $n = 121$, mean = 3.2 degrees) cells, (B) MGN ($n = 16$, mean = 11.5 degrees) and normal LGN ($n = 53$, mean = 2.5 degrees) cells with eccentricities less than 30 degrees, and (C) normal LGN cells shown by class [same data as in A: X, $n = 71$, mean = 2.6; Y, $n = 40$, mean = 4.0; W, $n = 10$, mean = 3.9 (does not include three W cells with unplotable receptive fields)].

(Mann-Whitney U, $P < .0001$). While neither X, Y, or W cells in the normal LGN exhibited receptive field sizes as large as some seen in the MGN, some LGN W cells (Fig. 6C) did have large receptive fields with diffuse borders ($n = 2$)

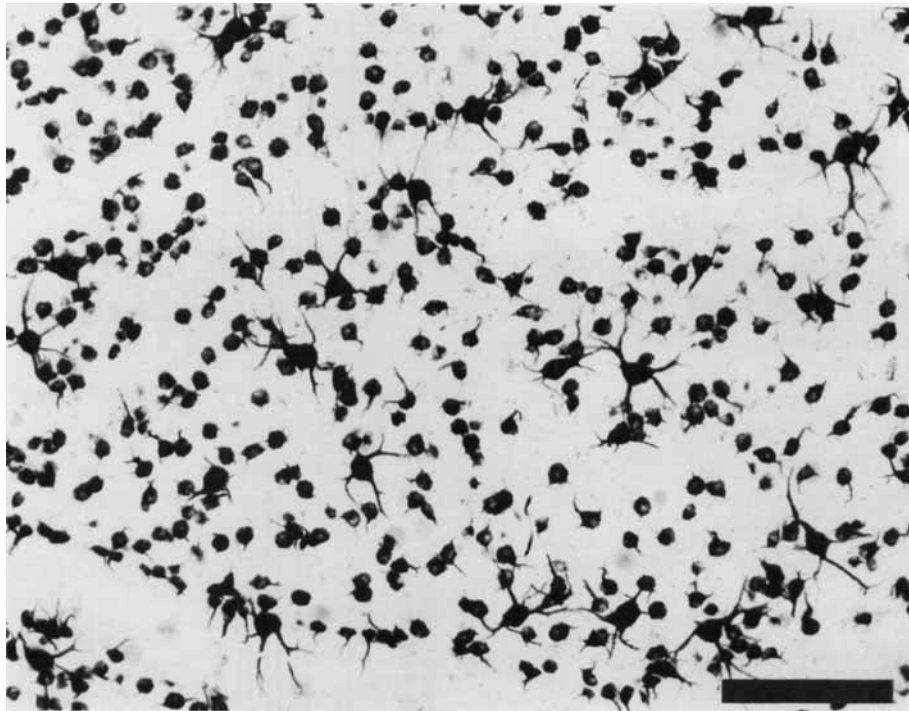


Fig. 7. Photomicrograph of retinal ganglion cells back-filled from a large injection of horseradish peroxidase (HRP) into the thalamus of a rewired (VCX + SC + BC) ferret (VCX, visual cortex; SC, superior colliculus; BC, brachium of the inferior colliculus). Cells with α morphologies are easily distinguishable. Cells are primarily small and large in size. Scale bar = 250 μm .

or receptive fields that were difficult to plot ($n = 3$) (cf. Cleland and Levick, '74a,b; Sur and Sherman, '82).

Responses to auditory stimulation. Auditory responsiveness of MGN cells ($n = 27$) was examined in two experiments on rewired animals. Responses to broad-band auditory stimuli such as clicks and white noise were obtained in some ($n = 4$) MGN cells. The physiological characteristics of auditory responses were not examined in further detail. A few ($n = 3$) MGN cells exhibited both visual and auditory responsiveness. In these cells, the response to stimulation of one modality (visual) dominated that of the other modality (auditory). While very few such cells were observed, the convergence of auditory and visual inputs onto single cells remains an intriguing developmental issue.

Retinal ganglion cells in rewired ferrets: morphological characteristics

Retinal ganglion cell morphologies. Retinal ganglion cells were labelled following large injections of HRP into thalami of normal ($n = 1$) and rewired ($n = 1$) ferrets. Retinal ganglion cell morphologies in normal ferrets were similar to those described previously in ferret retina (Henderson, '85; Vitek et al., '85). The retinal morphological cell types seen following thalamic injections in rewired ferrets were qualitatively indistinguishable from normal (Fig. 7). In retinæ of both normal and rewired ferrets, cells with α -like morphologies were most easily distinguished by their large, angular somatas and often extensively filled dendritic processes. Cells of the β cell class (fewer in rewired ferret retinæ; see below) were often identified by their round, medium-sized somata and typically a single prominent proximal dendrite. Other morphological cell

types were rarely distinguished due to the limited dendritic labelling of small and medium-sized cells.

Retinal ganglion cell soma sizes: large thalamic injections. Large thalamic injections of HRP (which also labelled optic tract fibers running toward the SC) in a normal and a rewired (VCX + SC + BC) ferret resulted in extensive labelling of both the contralateral retina and the temporal crescent of the ipsilateral retina, as has been described in detail previously (Morgan et al., '87). Retinal ganglion cells were well-labelled and soma sizes readily measured. For the purposes of discussion, we have divided the soma size distribution into small ($< 200 \mu\text{m}^2$), medium ($200\text{--}350 \mu\text{m}^2$), and large ($> 350 \mu\text{m}^2$) size ranges. We base the large soma size range on the percentage of α cells (approximately 5%) reported in the ferret retina (Vitek et al., '85). Our small soma size range was based on the small cells labelled from injections in the superficial SC [see below; cells projecting to the SC are primarily small (presumably W cells) or large (presumably Y cells) in size—this paper, Wingate et al., '90; cf. Leventhal et al., '85]. The medium size range (presumably X and perhaps some W cells) is simply the intermediate range between the small and the large. These cell size divisions are only meant as guides; the interpretation of our data is not critically dependent on the exact placement of these divisions.

In both normal and rewired ferret retinæ, soma size measurements ranged from less than $50 \mu\text{m}^2$ to more than $400 \mu\text{m}^2$ (Fig. 8A). In the normal ferret (white bars), 48%, 46%, and 6% of the back-filled retinal ganglion cells fell into the small, medium, and large categories, respectively. Soma sizes back-filled from the rewired (black bars) thalamic injection were significantly smaller than normal (Mann-Whitney U, $P < 0.025$). In the rewired ferret, there is a

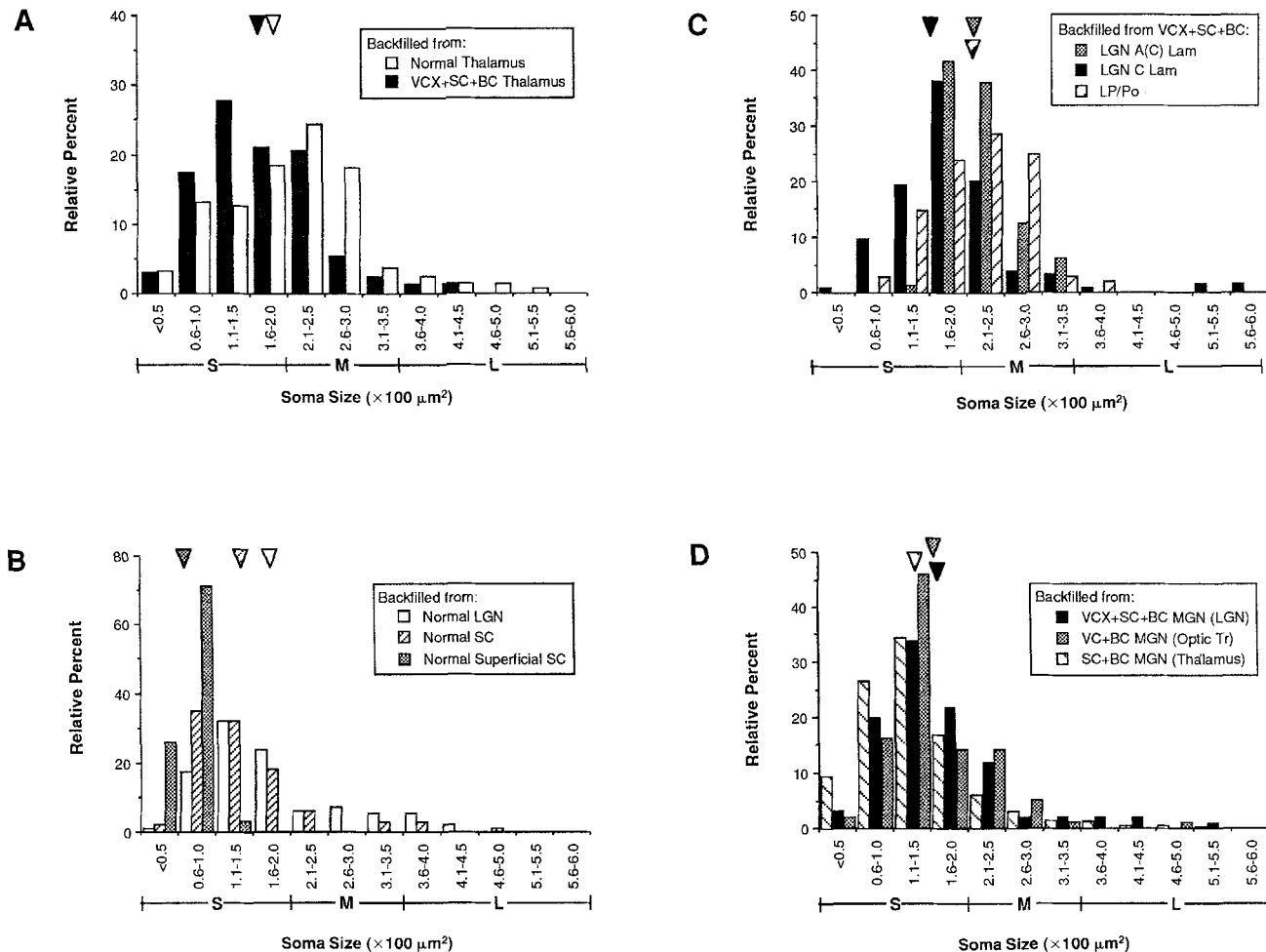


Fig. 8. Soma size distributions of retinal ganglion cells back-filled from thalamic injections of HRP. **A:** Total retinal ganglion soma size distribution (following large thalamic injections) in a normal animal (white bars, mean = 190 μm^2) and a VCX + SC + BC lesioned animal (black bars, mean = 173 μm^2). **B:** Soma size distributions of retinal ganglion cells projecting to LGN (white bars, mean = 178 μm^2), SC (hatched bars, mean = 146 μm^2), and upper superficial SC (gray bars, mean = 67 μm^2) in normal ferrets. **C:** Soma size distributions of retinal

ganglion cells projecting primarily to the A laminae of the LGN (gray bars, mean = 222 μm^2), the C laminae of the LGN (black bars, mean = 162 μm^2), and the lateral posterior nucleus/posterior thalamic group (LP/Po) complex (hatched bars, mean = 218 μm^2) in VCX + SC + BC lesioned ferrets. **D:** Soma size distributions of retinal ganglion cells projecting primarily to the MGN of VCX + SC + BC (black bars, mean = 165 μm^2), VCX + BC (gray bars, mean = 162 μm^2), and SC + BC (hatched bars, mean = 141 μm^2) lesioned ferrets.

marked reduction in the number of medium-sized retinal ganglion cells (from 46% to 28%). This is consistent with the significant retinal X cell loss (Tong and Spear, '82; cf. Sur et al., '87) as well as medium-sized W cell loss (Rowe, '90) found in cats with neonatal visual cortical ablations.

Retinal ganglion soma sizes: restricted injections. To address more specifically which retinal ganglion cell populations comprise these distributions, restricted injections were made into retinal target zones of normal and rewired animals.

Normal animals. In normal animals, restricted injections into the LGN (n = 1) resulted in labelling of small (74%), medium (19%), and large (7%) soma sizes (Fig. 8B, white bars). Similar to retinal projections to the SC in the cat, SC-projecting cells in the ferret (n = 1) were primarily small (87%) or large (4%) in size (Fig. 8B, hatched bars). A small injection restricted to the most superficial layer of the SC superficial grey (n = 1) labelled almost exclusively (97%) cells in the extremely small (< 100 μm^2) cell size range (Fig. 8B, gray bars); in contrast, only 18% of the cells

back-filled from the LGN were smaller than 100 μm^2 . Thus, similar to retinal projections in the cat, it is likely that W cells projecting to the superficial SC are smaller in size than those projecting to the C laminae of the LGN (Leventhal et al., '85; Stanford, '87a).

In rewired (VCX + SC + BC) ferrets, restricted injections into the LGN revealed somewhat different retinal soma size distributions. An injection centered in the A lamina and impinging on the C lamina (Fig. 9A) labelled small (43%, mostly > 150 μm^2) and medium (57%) sized cells (Fig. 8C, gray bars). In another rewired ferret, an injection almost entirely restricted to the C lamina (with some encroachment into the optic tract; Fig. 9B) labelled many more small cells (68%, mostly > 100 μm^2) as well as some large (6%) cells (Fig. 8C, black bars). The results from these two LGN injections suggest that in rewired ferrets the remnant retinal projection to the C laminae of the LGN consists of both Y and larger sized W input. Labelling of medium-sized cells from the A lamina injection may repre-

sent surviving β cells (Sur et al., '87b). In a third rewired ferret, a restricted injection was made in the lateral posterior nucleus/posterior thalamic group (LP/Po) complex (Fig. 9C). The soma size distribution resulting from this injection is shifted towards medium sized cells (57%; Fig. 8C, hatched bars). The enhanced projection to LP/Po previously described in rewired ferrets (Pallas et al., '90) is thus likely to be comprised of larger W or remaining X retinal ganglion cells.

In contrast, retinal ganglion cells projecting to the MGN of rewired ferrets are primarily small in size (Fig. 8D). A restricted injection (which abutted the overlying LGN; Fig. 9D) was made into the MGN of a rewired (VCX + SC + BC) ferret. The retinal soma size distribution resulting from this injection is clearly shifted towards smaller soma sizes (Fig. 8D, black bars): almost 80% fall in the small cell range, approximately 30% of which are $< 100 \mu\text{m}^2$ and 70% of which are $> 100 \mu\text{m}^2$. Projections to the MGN in rewired ferrets with other combinations of lesions are also similar, at least qualitatively (Fig. 8D; see also below).

In summary, the distribution and projection patterns of small, medium, and large retinal ganglion cells in the normal ferret retina are consistent with those found in previous studies in ferret and in cat. Roughly speaking, the LGN A laminae receive X and Y cell input, LGN C laminae primarily Y and medium sized W cell input, and the SC primarily Y and small sized W input. Retinal ganglion cells projecting to the MGN of rewired ferrets are primarily small in size, overlapping in size with those of normal SC-projecting W cells (primarily $< 100 \mu\text{m}^2$) as well as normal LGN C laminae-projecting W cells (primarily $> 100 \mu\text{m}^2$). Thus, the anatomical soma-size data suggest that W cells may be a major source of input to the MGN in rewired ferrets.

Retinal ganglion cell plasticity in rewired ferrets: selective redirection of ganglion cell subpopulations

Given the known diversity of the W cell class, we were curious as to whether we could selectively induce subpopulations of these cells to innervate the MGN. W cell subpopulations in the normal cat visual system have specific retinofugal projection patterns. We reasoned that by selectively removing or reducing only one of the two major W cell target zones (the LGN and the SC) early in development, we could selectively reroute specific W cell subpopulations. We were also interested in exploring how the availability of alternative target space influenced the rerouting of these subpopulations.

We have therefore examined the retinal ganglion cell soma sizes as well as retinal terminal projections in ferrets that had received different combinations of the following three lesions on the day of birth: visual cortical lesion (VCX, which leads to extensive LGN degeneration), superior colliculus lesion (SC), and transection of the brachium of the inferior colliculus (BC). Making different combinations of lesions might vary the size of the retino-MGN projection based on removal of the normal targets of each subpopulation. Ferrets with the following combinations of lesions were studied: VCX + SC + BC, SC + BC, VCX + BC, VCX + SC, VCX, SC, BC; their retino-MGN projections were compared with each other, and the retinal ganglion cell populations compared with those in normal ferrets.

Retinal projections to MGN. In normal ferrets, the LGN and the SC are the major retinal target zones. The laminar

pattern of innervation seen in the LGN (Fig. 10A) is typical of the carnivore LGN: the A and the dorsal C laminae receive contralateral input, and the A1 (and C1) laminae receive ipsilateral input. The MGN receives no retinal input (Fig. 10A). In ferrets that received a full complement of VCX, SC, and BC lesions (VCX + SC + BC) at birth, a significant projection to the MGN can be established, though there is variability in the extent of projection. In these animals, retinal afferents terminate in almost all divisions of the MGN, including the dorsal, ventral, and medial divisions as defined by Morest ('65) (Figs. 10B, 11). The caudal-most portion of the MGN, which in normal animals does not project to primary auditory cortex (Aitkin et al., '84), never receives retinal input. Unlike the retino-LGN projection, retinal afferents to the MGN terminate in a patchy fashion (Figs. 10B, 11). Often fibers are seen streaming into the MGN from the ventral optic tract at the base of the LGN or from the dorsocaudal border of the MGN.

Ferrets that receive less than the full complement of lesions at birth also demonstrate aberrant induction of retinal terminations; however, the size of the projection is significantly smaller. Ferrets that have only the SC and BC lesions (SC + BC, $n = 3$) also received retinal input to the ventral, dorsal, and medial divisions of the MGN; however, the extent of these projections to the MGN were much smaller in comparison (Fig. 10C). Ferrets that received only VCX and BC lesions (VCX + BC, $n = 3$) at birth exhibited the least extensive retino-MGN projections (Fig. 10D).

To quantify these impressions, we mapped the regions of retinal termination (both heavy and light) in the MGN and calculated the extent of retinal termination in the MGN as a percent of total MGN volume in each animal. In the example shown in Figure 11 (a VCX + SC + BC case), the volume of retinal termination in the MGN is 0.47 mm^3 , the total MGN volume is 1.70 mm^3 (though a part of the MGN itself has been lesioned) and the resulting innervated MGN volume is 28%. Figure 12 illustrates the result of such calculations for ferrets that had undergone different lesion combinations as neonates. The heaviest retinal innervation is seen in the two VCX + SC + BC animals in which 28% and 17%, respectively, of the MGN contained retinal label. In three SC + BC lesioned animals, 8%, 6%, and 2%, respectively, of the MGN contained retinal label. Only 0.5%, 1.2%, and 1.2% of the MGN volumes in the three VCX + BC animals, respectively, contained label.

No innervation of the MGN was seen in ferrets that did not receive brachium transection (VCX, $n = 1$; SC, $n = 2$; VCX + SC, $n = 1$), nor did the BC lesion alone ($n = 1$) induce MGN innervation. Thus, it appears that the VCX lesion and the SC lesion when done in conjunction with the brachium transection is the most effective for induction of retinal afferents into the MGN. One reason for variability in the retino-MGN projections is thus the completeness of the various lesions, and this is an issue that warrants further study (see Discussion).

We make three observations about these findings: 1) denervation of the MGN is a *necessary, but not sufficient* condition for retinal afferent induction; 2) when done in conjunction with the brachium transection, either the VCX or SC lesion alone is *sufficient* for induction of some afferents; and 3) the inductive effect of VCX + SC + BC lesions is much larger than the sum of VCX + BC and SC + BC lesions. The interpretation of these results and their

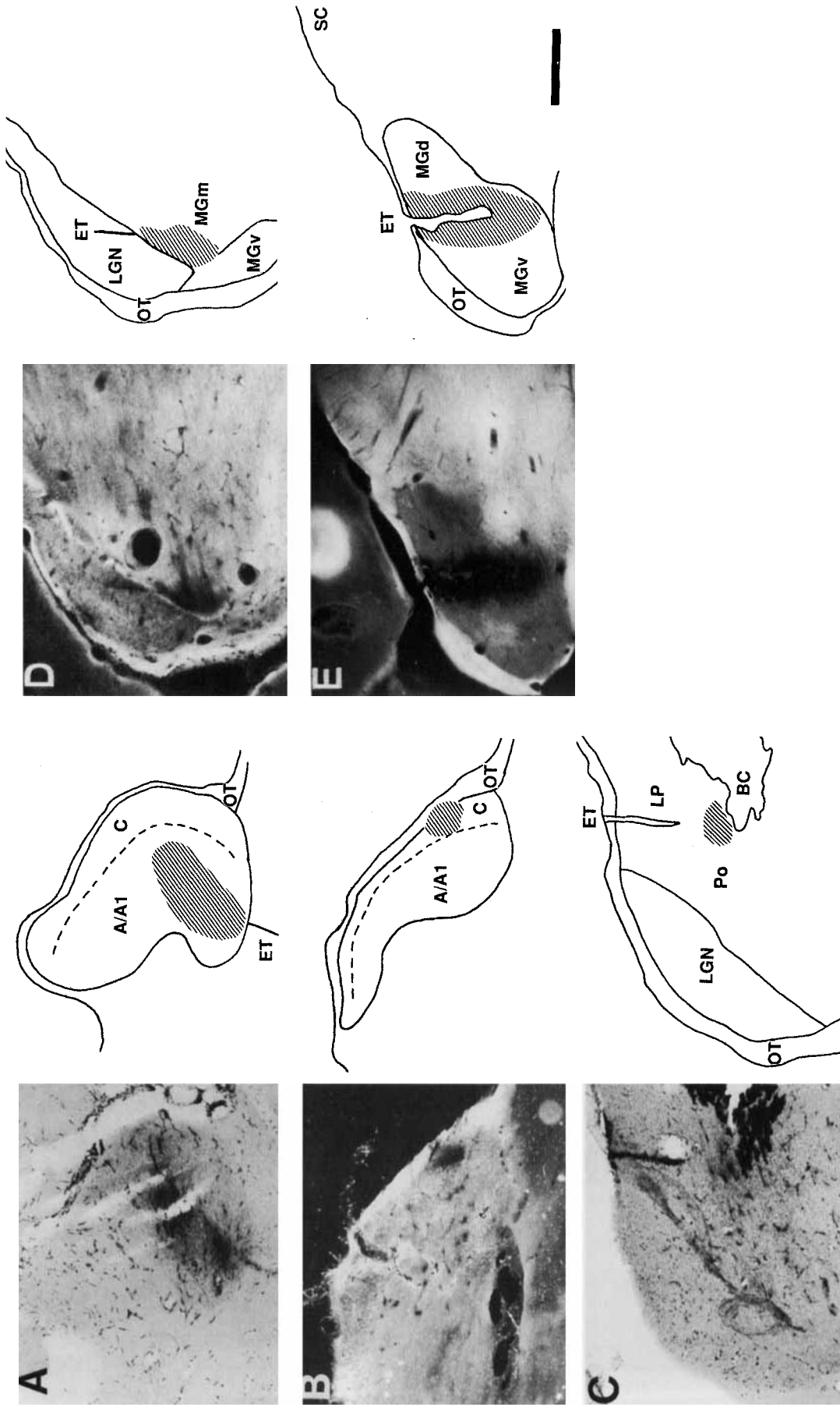


Fig. 9. Restricted HRP injection sites in VCX + SC + BC (A-D) and in VCX + BC (E) lesioned ferrets producing the retinal back-fills presented in Figure 8C and D. Sections are shown in photomicrographs on the left with explanatory drawings on the right (injection site indicated by hatched lines). **A:** An injection centered in the A laminae and impinging on the C laminae (C) of the LGN (see Fig. 8C, gray bars). **B:** An injection restricted to the LGN C laminae (see Fig. 8C, black bars). **C:** An injection into LP/Po complex (see Fig. 8C, hatched bars). **D:** An injection into the MGN (see Fig. 8D, black bars). There is some spread of label into the LGN above. **E:** An injection into the MGN with some encroachment into the optic tract (see Fig. 8D, gray bars). ET, electrode track. OT, optic tract. BC, blood clot. Scale bar = 500 μ m and applies to A-E.

Fig. 9. Restricted HRP injection sites in VCX + SC + BC (A-D) and in VCX + BC (E) lesioned ferrets producing the retinal back-fills presented in Figure 8C and D. Sections are shown in photomicrographs on the left with explanatory drawings on the right (injection site indicated by hatched lines). **A:** An injection centered in the A laminae and impinging on the C laminae (C) of the LGN (see Fig. 8C, gray bars). **B:** An injection restricted to the LGN C laminae (see Fig. 8C, black bars). **C:** An injection into LP/Po complex (see Fig. 8C, hatched bars). **D:** An injection into the MGN (see Fig. 8D, black bars). There is some spread of label into the LGN above. **E:** An injection into the MGN with some encroachment into the optic tract (see Fig. 8D, gray bars). ET, electrode track. OT, optic tract. BC, blood clot. Scale bar = 500 μ m and applies to A-E.

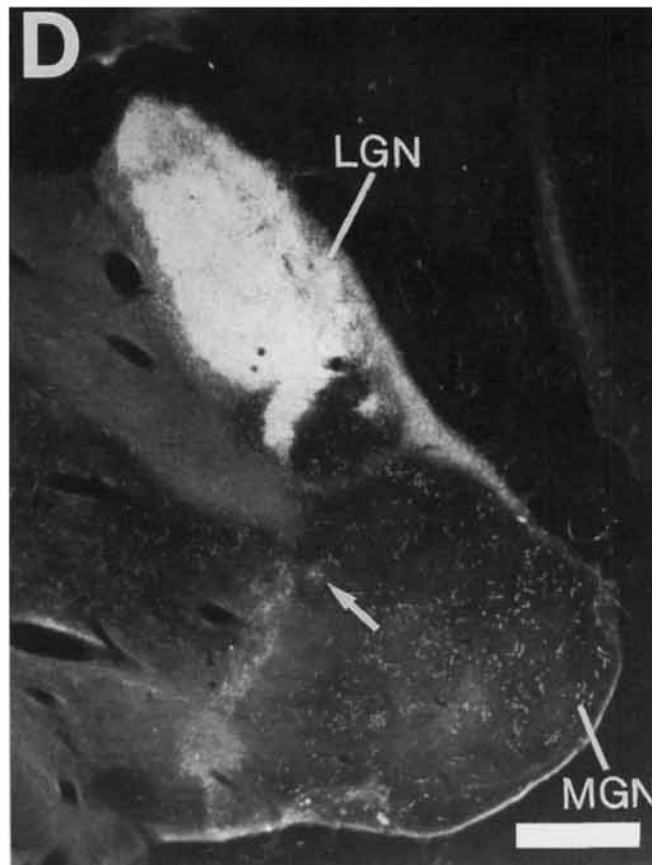
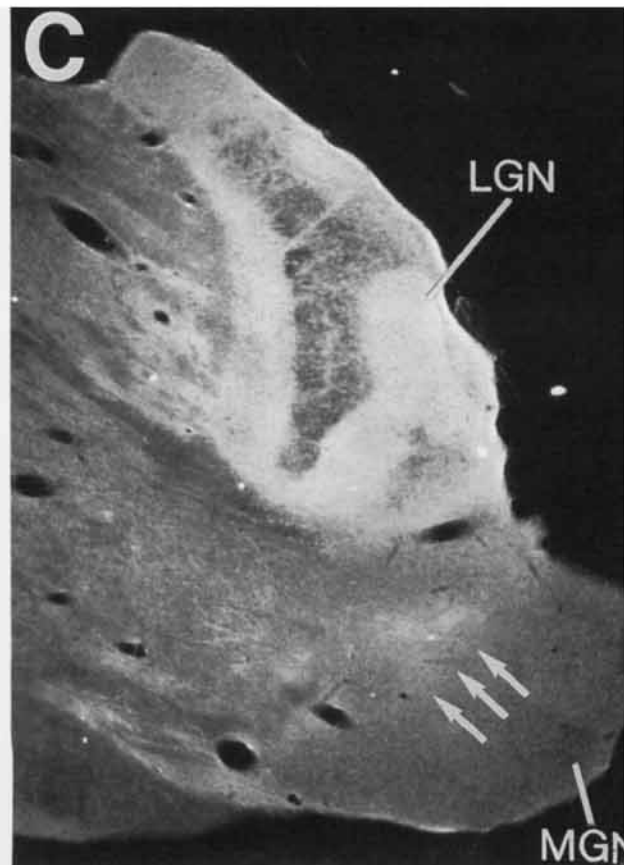
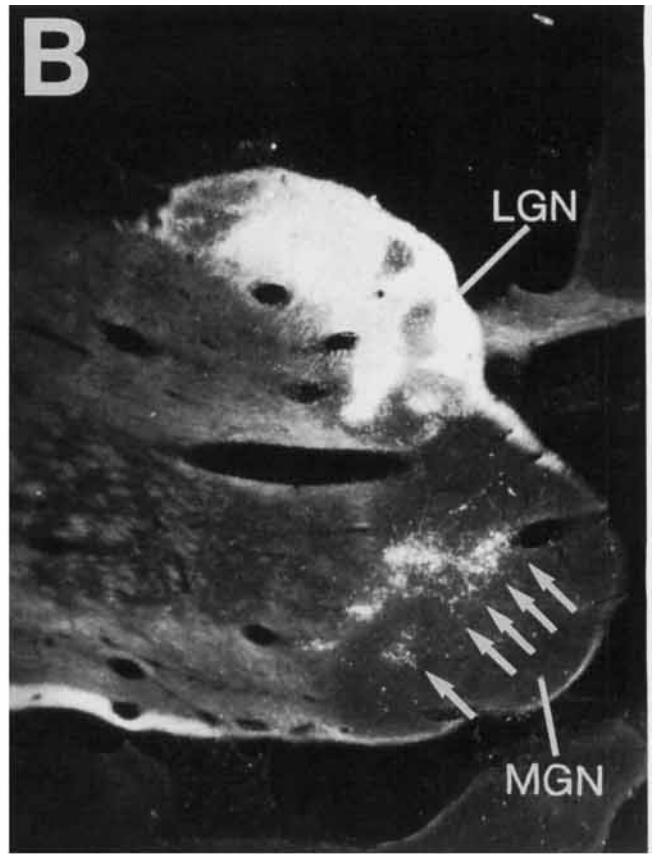
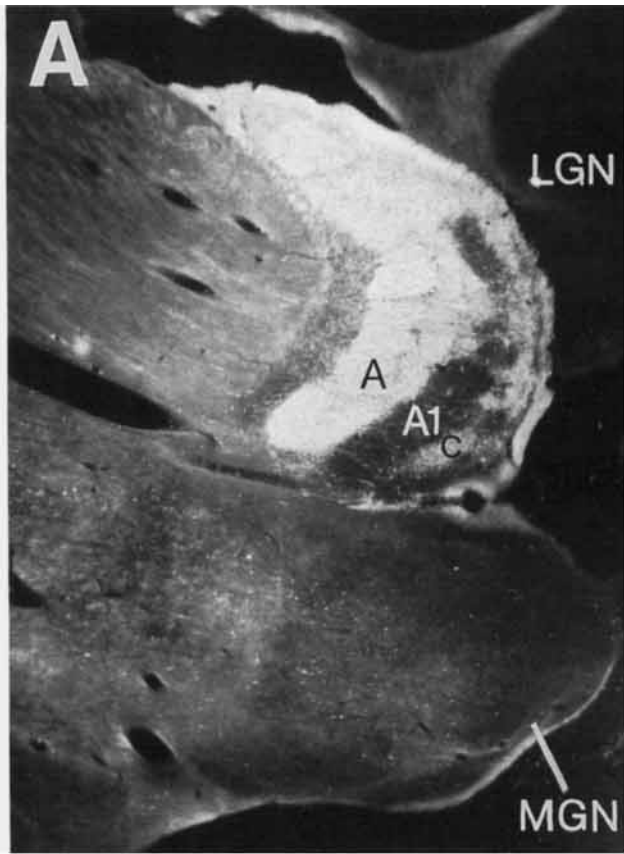


Figure 10

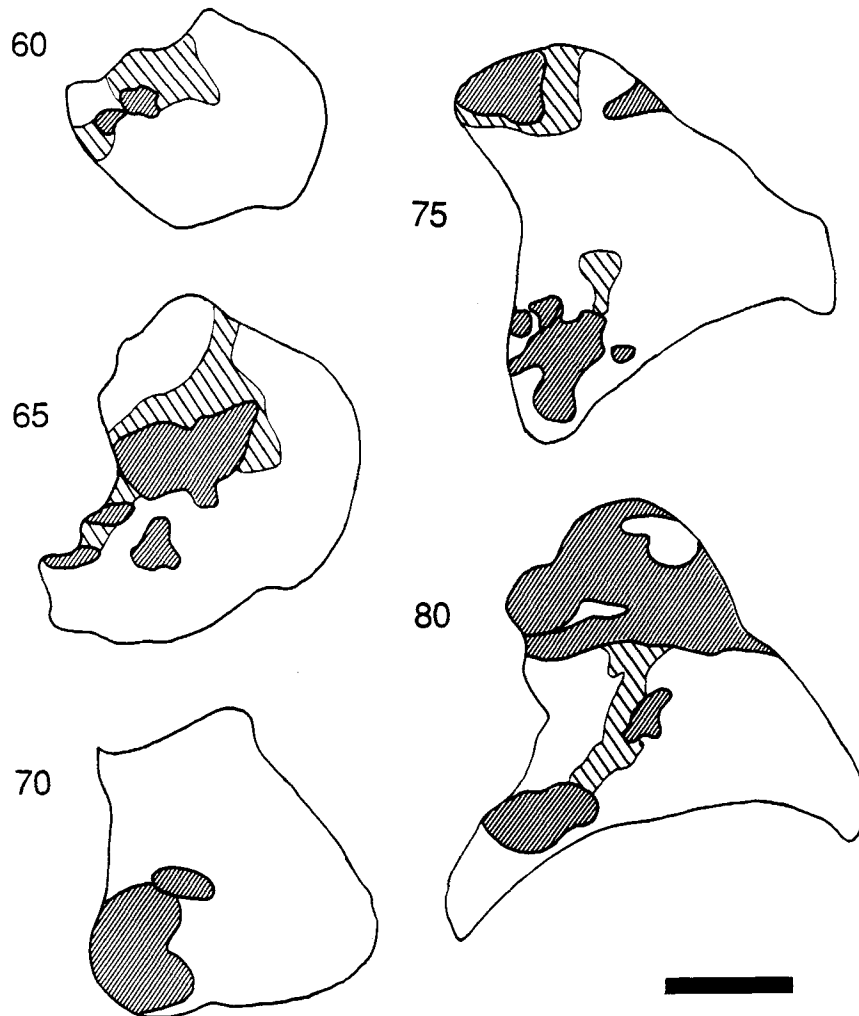


Fig. 11. Reconstruction of retinal terminal label in sagittal sections of the MGN in a rewired (VCX + SC + BC) ferret. Dense hatching indicates regions of heavy terminal label; more widely spaced hatching indicates regions of light label. Rostral is to left and dorsal is up. Section

numbers (each section $50\ \mu\text{m}$ thick) run from lateral (60) to medial (80). Patchy retinal terminal label is found in ventral, dorsal, and medial divisions of the MGN. Scale bar = $250\ \mu\text{m}$.

bearing on the retinal cell classes that project to the MGN will be examined in the discussion.

Retinal ganglion cell soma sizes. In one VCX + BC case, a restricted injection of horseradish peroxidase was

Fig. 10. Photomicrographs of sagittal sections through the LGN and MGN of normal and rewired ferrets that have received an injection of HRP-WGA in the contralateral eye. Dorsal is up and rostral to left. **A:** Normal adult ferret. Laminae A and C are well delineated. MGN is devoid of label. **B:** Adult ferret that received neonatal lesions of visual cortex, superior colliculus, and brachium of inferior colliculus (VCX + SC + BC). Remnant LGN, retaining retinal afferents, is shrunken in size and displays abnormal lamination pattern. In contrast to the normal MGN, MGN in rewired ferrets receive substantial amount of retinal input. Arrows indicate label in the MGN. **C:** Adult ferret that received only SC + BC lesions at birth. LGN is normal in size and lamination. MGN also contains retinal terminal label (marked by arrows), but to a lesser degree than in VCX + SC + BC animals. **D:** Adult ferret that received only VCX + BC lesions at birth. LGN is shrunken in size. MGN contains much less retinal innervation than in VCX + SC + BC animals (small zone of retinal termination indicated by white arrow). Note white matter and blood vessel artifacts that can also appear white in these photomicrographs are clearly distinguished from terminal label. Scale bar = $500\ \mu\text{m}$ and applies to A-D.

made in the MGN (impinging slightly on the optic tract, Fig. 9E). The retinal ganglion cell size distribution back-filled from this injection is shown in Figure 8D (gray bars). This distribution consists of almost 80% small cells, 76% of which are $> 100\ \mu\text{m}^2$ in size (Fig. 8D, gray bars) and is not significantly different from that resulting from an MGN injection in the VCX + SC + BC case (compare with Fig. 8D, black bars; Mann-Whitney U, $P > 0.3$).

We attempted to make a restricted injection of horseradish peroxidase in the MGN of a SC + BC case. This injection (not shown), while exhibiting significant diffusion away from the injection site, was centered in the MGN. When back-filled retinal ganglion cell soma sizes were measured (shown in Fig. 8D, hatched bars), 88% of the soma sizes are small, of which 41% are $< 100\ \mu\text{m}^2$ in size. These soma sizes are significantly smaller (Mann-Whitney U, $P < 0.002$) than those in the VCX + BC case (compare Fig. 8D, gray bars).

In summary, in both VCX + BC and SC + BC lesioned ferrets, the retinal ganglion cells innervating the MGN are small in size. Furthermore, those projecting to the MGN in SC + BC animals tend to be smaller in size (41% < 100

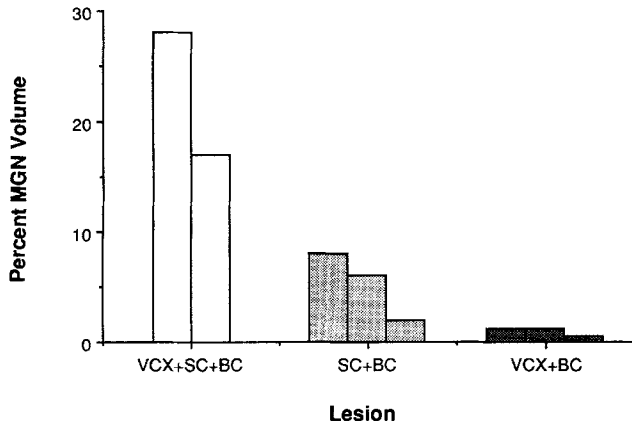


Fig. 12. Size of retino-MGN projection expressed as a percent of MGN volume for each of the animals that received VCX + SC + BC lesions ($n = 2$), SC + BC lesions ($n = 3$), or VCX + BC lesions ($n = 3$) at birth. Volumes calculated from areal measurements of drawings such as those shown in Figure 11; retinal projection areas include regions of both dense and light hatching. Animals that received VCX + SC + BC lesions have the most extensive retinal projection to the MGN.

μm^2) than those projecting to the MGN in VCX + BC animals ($24\% < 100 \mu\text{m}^2$). These findings are consistent with the hypothesis that the W cell populations that undergo redirection into alternative target zones are those that are deprived of their normal targets (see Discussion).

DISCUSSION

Retinal ganglion cells projecting to MGN: a hypothesis

Each physiological class of ganglion cell in the cat retina possesses a distinct morphology (Stone and Clarke, '80; Fukuda et al., '84; Stanford and Sherman, '84; Stanford, '87a,b), retinal distribution (Stone, '78; Wässle and Illing, '80; Leventhal, '82), and central projection pattern (Kelly and Gilbert, '75; Leventhal et al., '85). The ferret retina contains ganglion cell types similar to those in the cat but in somewhat different proportions: the ferret retina contains ganglion cells with large alpha-type somata (Y cells, 5%), medium size beta-type somata (X cells, 25%), and other small and medium size somata (W cells, 70%) (Henderson, '85; Vitek et al., '85; Wingate et al., '90). There is good evidence that Y cells project primarily to the A, A1, and magnocellular C laminae of the LGN and the deeper part of the superficial SC. X cells project primarily to the A laminae of the LGN (Roe et al., '89).

Our current understanding of the projection patterns of retinal W cells in cats is schematized in Figure 13A. Medium sized W cells, which compose a significant proportion (30%) of the medium sized retinal ganglion cell population (Stanford, '87a), project primarily to the parvocellular C laminae of the LGN and the MIN (Rowe and Dreher, '82; Leventhal et al., '85). Small sized W cells project primarily to the dorsal superficial SC as well as to the ventral LGN and the pretectum (Hoffmann and Schoppmann, '75; Guillery and Oberdorfer, '77; Spear et al., '77; Wässle and Illing, '80). Some of these small cells (20%, Leventhal et al., '85; 43%, Illing and Wässle, '81) bifurcate to both the LGN and the SC (see Illing, '80 and Wingate et al., '90 for direct demonstration of bifurcating γ cells). One study demon-

strates (indirectly) dramatic loss of medium sized W cells following neonatal visual cortical ablations in cats (Rowe, '90); this would suggest that many cells that project to the C laminae of the LGN do not bifurcate.

In the present study, we suggest, by analogy with cats, that neonatal ablation of the SC (SC + BC) in ferrets deprives the SC-projecting (small) W cell population of its primary target, thereby inducing (we believe) these W cells to seek out alternative target space in denervated MGN territory (Fig. 13B). Similarly, neonatal ablation of the VCX (VCX + BC) most strongly deprives the C laminae-projecting (medium sized) W cells of their target, leading to selective redirection of this W cell population (Fig. 13C). Consistent with this scheme, we find that small cells projecting to the MGN in VCX + BC cases are somewhat larger than those labelled in SC + BC cases (Fig. 8D). When both lesions are done in conjunction (VCX + SC + BC), not only should the SC-projecting and the LGN-projecting W cell populations be affected but also the W cells, which project via a bifurcation to both the SC and the LGN (Fig. 13D). As a result, in VCX + SC + BC animals, the distribution of the retinal ganglion cells reflects both small and large W cell populations (Fig. 8D) and the extent of the aberrant projection to the MGN is correspondingly larger than the sum of projections in SC + BC and VCX + BC animals (Fig. 10B).

We must also consider other possible explanations of our findings. While we cannot entirely discount the possibility that a small number of the medium sized cells labelled are X cells, we have no compelling physiological indication that X cells contribute significantly to the MGN projection (see below). Better dendritic filling techniques than HRP backfills would be required to exclude this possibility. The substantially increased projection in VCX + SC + BC cases may also result from enlarged W cell terminal arbors in the MGN. However, labelling of single arbors arising from the optic tract and terminating in the MGN suggests otherwise (Pallas et al., '89, '91). Another possible explanation for the increased projection size in the VCX + SC + BC case is that removal of both the LGN and SC leads to survival of some cells that would have been lost following removal of either only VCX or SC. This might be achieved via reduction in intraretinal dendritic competition during the period of cell death (cf. Linden and Serfaty, '85).

We consider yet another explanation for these findings. Is it possible that some of the small soma sizes result from shrunken X or Y retinal ganglion cells? Consider the possibility that some X or Y cells have shrunken somata, consequently finer, more slowly conducting axons, and, furthermore, terminate in abnormal synaptic configurations that appear physiologically undifferentiable from W response characteristics. This is a possibility that is difficult to eliminate but equally difficult to establish. Without a definitive marker that tags "X-ness" or "Y-ness," it would be quite difficult to provide evidence supporting this hypothesis. Ultimately, this hypothesis may simply be a question of classification. Can a cell that has a small soma and a slowly conducting axon and that contributes to W-like postsynaptic responses be considered "X" or "Y"?

Physiological responses of MGN cells

In cats, W-type ganglion cells are actually a heterogeneous class composed of at least several subclasses (e.g., Stanford, '87a). W cells have poor, inconsistent (sluggish) responses to visual stimuli; either tonic (medium sized cells) or phasic (small sized cells) responsiveness; large

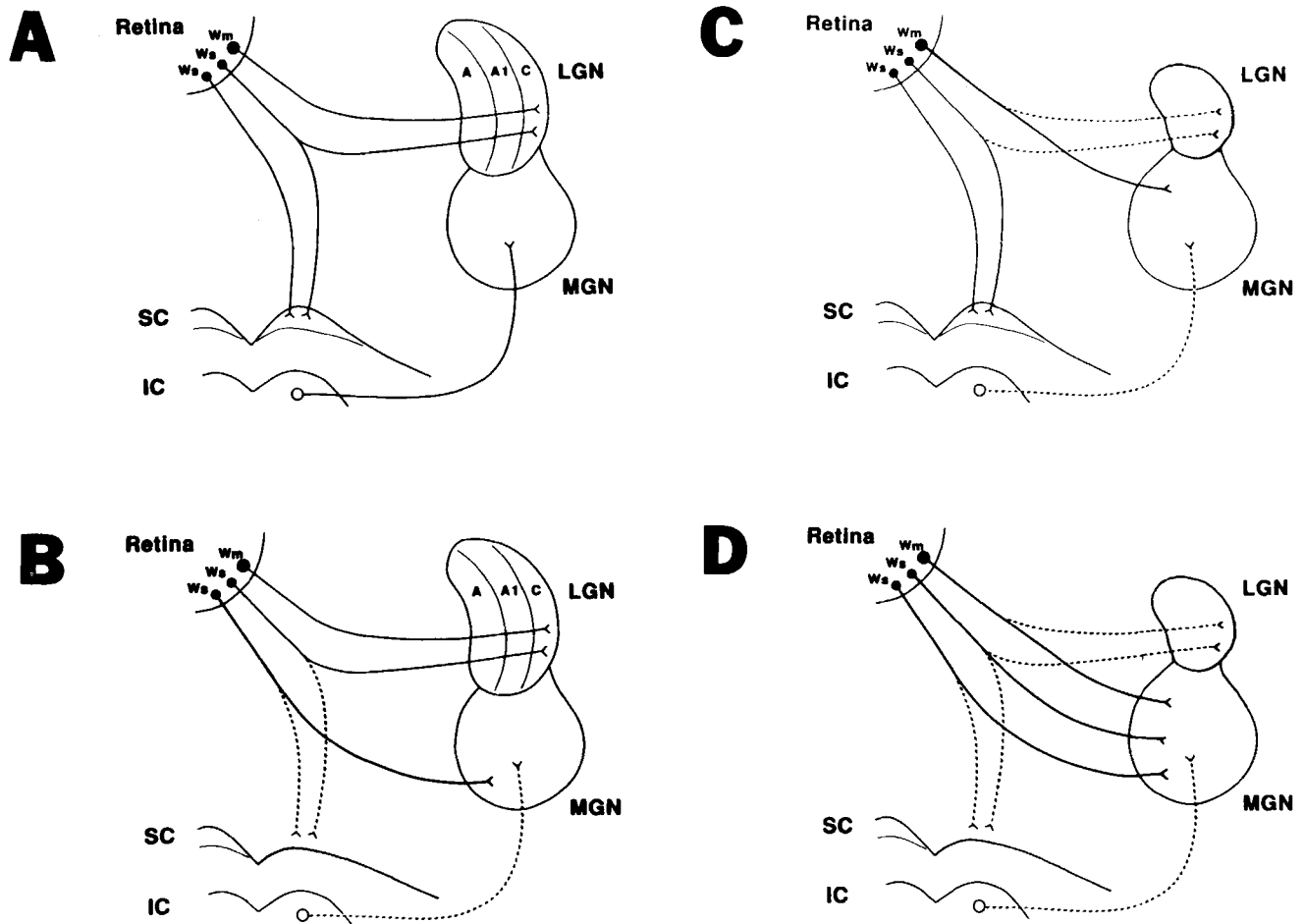


Fig. 13. Schematic diagram of retinal W cells and their central projection patterns in normal (A) and rewired (B–D) ferrets. **A:** In normal ferrets, medium sized W cells (W_m) project primarily to the LGN C laminae. Some small W cells (W_s) project to the dorsal superficial (SC); others project to both the (LGN) C laminae and SC via an axonal bifurcation. The MGN receives afferent input from the inferior colliculus (IC). **B:** In SC + BC ferrets, nonbifurcating small W cells, deprived of their normal target, reroute to the MGN. Solid lines indicate projec-

tions that remain; dotted lines indicate projections that are lost. **C:** In VCX + BC ferrets, medium sized W cells respond to reduction in C lamina target space by rerouting to available territory in the MGN. **D:** In VCX + SC + BC ferrets, all W cell populations depicted are affected by target zone reduction and therefore reroute to the denervated MGN. This results in a more extensive projection than in either the SC + BC or the VCX + BC cases and, in fact, greater than the sum of the SC + BC and VCX + BC cases.

receptive field sizes, some with center-surround organization and others with diffuse receptive fields; poor and either linear or nonlinear spatial summation; and thin, poorly myelinated, slowly conducting axons. Contrast preferences of W cells include on, off, on/off, contrast-suppressed, and color-coded types. Direction-selective W cells have also been described (Cleland and Levick, '74a,b; Wilson et al., '76; Rodieck, '79; Sur and Sherman, '82; Rodieck and Brening, '83; Fukuda et al., '84; Stanford, '87a).

The physiological response properties of visual cells in the MGN suggest that their visual input arises from retinal W cells. These cells have 1) long conduction latencies, indicating input from finely myelinated, slowly conducting retinofugal axons; 2) poor or sluggish responsiveness; 3) large receptive field sizes, some of which exhibit diffuse borders; 4) heterogeneity in stimulus preferences; and 5) the presence of some directionally selective cells.

Inferring presynaptic source from postsynaptic responses. In general, with our electrodes, retino-MGN axons were not encountered, either because of their small axon diameter or because of the sparseness of the projec-

tion. Even in normal ferrets, W retinogeniculate axons are rarely encountered during LGN or optic tract recordings, in contrast to X and Y retinogeniculate axons (Roe et al., '89). Our physiological data are, therefore, based on the characterizations of postsynaptic visual cells in the MGN.

Postsynaptic thalamic cells are likely to have response properties similar to those of their input retinal ganglion cells. LGN cells receive input from retinal ganglion cells of a single physiological class and thus exhibit response properties very similar to those of their afferent retinal ganglion cells (X and Y cells: Cleland et al., '71; Hochstein and Shapley, '76; Lehmkuhle et al., '80; So and Shapley, '81; W cells: Wilson et al., '76; Sur and Sherman, '82). These shared characteristics include nearly every major physiological feature described for retinal ganglion cells, such as center-surround organization of the receptive field, linearity of spatial and temporal summation, tonicity of center response, receptive field size, strength of surround suppression, response to large, fast-moving targets, and axon conduction velocity.

While our data are consistent with retinal W cell input to the MGN, we cannot ignore the possibility that some W-like physiological responses in the MGN may arise from the convergence of multiple retinal cell classes onto single MGN cells. We must also consider the possibility that the MGN does receive some retinal X or Y cell input, which, due to abnormal intrathalamic connectivity, leads to the observed W-like responses. We find this possibility unlikely for several reasons. First, intrathalamic synaptic connectivity seems to be a circuitry that is well conserved and rather ubiquitous across thalamic nuclei. For example, characteristic triadic arrangements of sensory input, projection cell, and local inhibitory input have been described in the LGN (Guillery, '69; Wilson et al., '84; Mize et al., '86), MGN (Morest, '75; Majorossey and Kiss, '76), and the ventrobasal nucleus (Penny et al., '83; Spreafico et al., '83). Electron microscopic evidence from hamsters in which retinal projections were routed to the somatosensory or auditory thalamus (Campbell and Frost, '88) also suggests that the intra-MGN circuitry in rewired ferrets is likely to be similar to that of the normal MGN. Second, Y cell input to the MGN is incompatible with the long afferent conduction latencies of MGN cells and small retinal ganglion cell soma sizes back-filled from the MGN. We have, furthermore, demonstrated that slow afferent conduction velocity is not due to a general, nonspecific effect on conduction latencies in rewired ferrets (Fig. 1C). Third, the overlap between X cell and W cell latencies and soma sizes raises the possibility that X cells contribute to the retino-MGN projection; however, this also appears to be unlikely based on the extensive X cell loss following visual cortical ablation and the physiological responses of visual cells recorded in the MGN.

A more direct means of establishing whether only W retinal ganglion cells project to the MGN is to characterize their dendritic morphology more completely. Such experiments would involve intracellularly labeling retinal ganglion cells previously identified as projecting to the MGN.

Plasticity in retinal projections to the MGN: conditions

The absence of a transient retinal projection to the MGN in neonatal ferrets (Hahm, '91) indicates that this aberrant retino-MGN projection is due to reactive sprouting and not to stabilization of a pre-existing exuberant projection (cf. Frost, '82, '84, '86). Under what conditions do retinal ganglion cell axons, presumably of the W type, sprout to innervate a novel target such as the MGN?

Our experiments suggest that there are necessary and sufficient conditions for such sprouting to take place. The two minimal conditions are: 1) reduction or removal of normal target zones; and 2) availability of alternative target space. Either of these conditions alone is not sufficient to induce retinal afferents to the MGN. Specifically, we suggest that removal/reduction of the SC or the LGN (in conjunction with deafferentation of the MGN) results in selective rerouting of the SC-projecting or the LGN-projecting W cell populations, respectively. It is also possible that lesions reducing terminal space in both SC and LGN additionally induce redirection of W cells with axons bifurcating to both SC and LGN; partial deprivation (i.e., lesion of either collateral) may not be sufficient to cause extensive rerouting of this population.

There is evidence that the availability of alternative target space is crucial for a retinal ganglion cell's survival.

Extensive removal of normal target zones without making available alternative target space leads to extensive cell death of affected retinal ganglion cells. Thus, neonatal ablation of visual cortex leads to extensive X cell death in both LGN and retina of cats (Murphy and Kalil, '79; Tong and Spear, '82; Callahan et al., '84; Payne et al., '84); medium sized retinal W cells are also lost (Rowe, '90). Y cells survive such lesions, presumably because they are maintained by other sustaining collaterals (for example, to the SC). We note that the smaller projection to MGN established following VCX + BC lesions than following SC + BC lesions may be due to the fact that usually a remnant portion of the LGN remains following neonatal visual cortical lesions (due to projections from the LGN to nonablated visual cortical areas), while tectal lesions remove the superficial SC entirely.

These observations are consistent with the "conservation of arbor principle" (Schneider, '73; Jhaveri et al., '91), that is, reduction of a cell's arbor size is accompanied by compensatory sprouting elsewhere in the arbor, either in a pre-existing collateral or at any point along an axon's trajectory where there is available terminal space (e.g., in LP/Po or even in a nonvisual structure such as the MGN). Indeed, we have found that the course of the optic tract in rewired ferrets is much more expanded than normal (Pallas et al., '89), extending over the surface of the MGN instead of remaining restricted over the LGN surface, something not seen in normal neonatal ferrets (Hahm, '91). This observation is consistent with compensatory reactive sprouting of retinal ganglion cell axons.

Plasticity in retinal W cell projections: developmental issues

Why might retinal W cells (and not X or Y cells) innervate the MGN? One possibility is that at the time of lesions W cells are the most able to reroute their axons. To obtain successful rerouting of retinal ganglion cell projections, lesions must be done at an early stage of retinofugal development: no retinal innervation of the MGN results from lesions done past P1 (unpublished observations). In the cat, medium sized retinal ganglion cells are generated from E21 to E31, large cells from E25 to E31, and small cells from E21 to E36 (Walsh et al., '83). Ferret retinal ganglion cells are generated during approximately the same period (Greiner and Weidman, '81). At birth (E41), retinal afferents have entered the LGN (Linden et al., '81; Hahm, '91) and the SC (A.W. Roe, unpublished observations; cf. Williams and Chalupa, '82), but have not yet segregated into eye-specific zones. The small cells that are among the last to be generated in the retina may, at the time of lesioning, still be developmentally susceptible to environmental influences with respect to their targeting decisions and may be thus be most able to innervate alternative targets (cf. Perry and Cowey, '82). In this view, lesions done earlier (prenatally) might enable X or Y retinal cells to project to the MGN as well.

An alternative explanation for the selective induction of W cell fibers into the MGN is that W cells are intrinsically different in their developmental program than X or Y cells. Thus, W cells could simply be less selective in target selection than X or Y cells when choices are available. In anecdotal support of this view, W cells innervate multiple thalamic and midbrain nuclei, whereas Y cells, and even more so X cells, target fewer structures. Although there are no studies on the development of W cell terminations, there

is substantial evidence that X and Y cells differ in their developmental programs (Sur et al., '84; Garraghty et al., '86a,b, '88, '89; for review, see Sur, '88; Garraghty and Sur, '88). Thus, it is possible that W cells have intrinsically different developmental capabilities as well. In this case, lesions performed earlier would not lead to X and Y cells innervating the MGN.

CONCLUSIONS

Based on the physiology of visual cells in the MGN, the anatomical soma size distributions of MGN-projecting cells, and the selective patterns of the rewired projection, we suggest that primarily retinal W cells reroute to the MGN in rewired ferrets. We cannot eliminate the possibility (and indeed, it would be quite difficult to establish) that these projections arise from shrunken X- or Y-type retinal ganglion cells with poorly myelinated axons that terminate in the MGN in abnormal synaptic configurations. However, we think that the most parsimonious and self-consistent interpretation of these data is that W retinal ganglion cells contribute strongly to the retinal projection to the MGN in rewired ferrets. In this view, it is possible to consider this visual pathway through auditory thalamus and cortex in rewired ferrets a "W cell pathway." These data bear significantly on the interpretations of subsequent cortical transformations in this pathway as well as their establishment during development (Roe et al., '90, '92).

ACKNOWLEDGMENTS

We thank Jong-On Hahm for participating in some of the experiments, Sarah L. Pallas for comments on manuscript, and Teresa Sullivan for excellent technical assistance. Supported by Whitaker Foundation (A.W.R.) and NIH grant EY07719 (M.S.).

LITERATURE CITED

- Aitkin, L.M., D.R.F. Irvine, and W.R. Webster (1984) Central neural mechanisms of hearing. In I. Darian-Smith (ed): *Handbook of Physiology*, Vol. III. Washington, DC: American Physiological Society, pp. 675-737.
- Berson, D.M. (1987) Retinal W-cell input to the upper superficial gray layer of the cat's superior colliculus: A conduction-velocity analysis. *J. Neurophysiol.* 58:1035-1051.
- Callahan, E.C., L. Tong, and P.D. Spear (1984) Critical period for the marked loss of retinal X-cells following visual cortex damage in cats. *Brain Res.* 323:302-306.
- Campbell, G., and D.O. Frost (1988) Synaptic organization of anomalous retinal projections to the somatosensory and auditory thalamus: Target-controlled morphogenesis of axon terminals and synaptic glomeruli. *J. Comp. Neurol.* 272:383-408.
- Cleland, B.G., and W.R. Levick (1974a) Brisk and sluggish concentrically organized ganglion cells in the cat's retina. *J. Physiol. Lond.* 240:421-456.
- Cleland, B.G., and W.R. Levick (1974b) Properties of rarely encountered types of ganglion cells in the cat's retina and an overall classification. *J. Physiol. Lond.* 240:457-492.
- Cleland, B.G., M.W. Dubin, and W.R. Levick (1971) Sustained and transient neurones in the cat's retina and lateral geniculate nucleus. *J. Physiol. Lond.* 217:473-496.
- DeOlmos, J.S. (1977) An improved HRP method for the study of central nervous connections. *Exp. Brain Res.* 29:541-551.
- Felleman, D.J., and D.C. Van Essen (1987) Receptive field properties of neurons in area V3 of Macaque monkey extrastriate cortex. *J. Neurophysiol.* 57:889-920.
- Frost, D.O. (1982) Anomalous visual connections to somatosensory and auditory systems following brain lesions in early life. *Dev. Brain Res.* 3:627-635.
- Frost, D.O. (1984) Axonal growth and target selection during development: Retinal projections to the ventrobasal complex and other "nonvisual" structures in neonatal Syrian hamsters. *J. Comp. Neurol.* 230:576-592.
- Frost, D.O. (1986) Development of anomalous retinal projections to nonvisual thalamic nuclei in Syrian hamsters: A quantitative study. *J. Comp. Neurol.* 252:95-105.
- Fukuda, Y., C.F. Hsiao, M. Watanabe, and H. Ito (1984) Morphological correlates of physiologically identified Y-, X-, and W-cells in cat retina. *J. Neurophysiol.* 52:999-1013.
- Garraghty, P.E., and M. Sur (1988) Interactions between retinal axons during development of their terminal arbors in the cat's lateral geniculate nucleus. In M. Bentivoglio and R. Spreafico (eds): *Cellular Thalamic Mechanisms*. New York: Elsevier, pp. 465-477.
- Garraghty, P.E., M. Sur, R.E. Weller, and S.M. Sherman (1986a) Morphology of retinogeniculate X and Y axon arbors in monocularly enucleated cats. *J. Comp. Neurol.* 251:198-215.
- Garraghty, P.E., M. Sur, and S.M. Sherman (1986b) Role of competitive interactions in the postnatal development of X and Y retinogeniculate axons. *J. Comp. Neurol.* 251:216-239.
- Garraghty, P.E., C.J. Shatz, D.W. Sretavan, and M. Sur (1988) Axon arbors of X and Y retinal ganglion cells are differentially affected by prenatal disruption of binocular inputs. *Proc. Natl. Acad. Sci. USA* 85:7361-7365.
- Garraghty, P.E., A.W. Roe, Y.M. Chino, and M. Sur (1989) Effects of convergent strabismus of the development of physiologically identified retinogeniculate axons in cats. *J. Comp. Neurol.* 289:202-212.
- Greiner, J.V., and T.A. Weidman (1981) Histogenesis of the ferret retina. *Exp. Eye Res.* 33:315-332.
- Guillery, R.W. (1969) The organization of synaptic interconnections in the laminae of the dorsal lateral geniculate nucleus of the cat. *Z. Zellforsch.* 96:1-38.
- Guillery, R.W., and M.D. Oberdorfer (1977) A study of fine and coarse retino-fugal axons terminating in the geniculate C laminae and in the medial interlaminar nucleus of the mink. *J. Comp. Neurol.* 176:515-526.
- Hahm, J. (1991) Influence of the target on the development of the ferret retinogeniculate projection. Doctoral dissertation, M.I.T., Cambridge, MA.
- Hahm, J., A.W. Roe, S.L. Pallas, and M. Sur (1989) Physiologically identified retinogeniculate X axons in ferrets with neonatal ablation of visual cortex: Sizes of terminal arbors depend only partly on target size. *Soc. Neurosci. Abstr.* 15:495.
- Henderson, Z. (1985) Distribution of ganglion cells in the retina of adult pigmented ferret. *Brain Res.* 358:221-228.
- Hochstein, S., and R.M. Shapley (1976) Quantitative analysis of retinal ganglion cell classifications. *J. Physiol.* 262:237-264.
- Hoffmann, K.-P. (1973) Conduction velocity in pathways from retina to superior colliculus in the cat: A correlation with receptive field properties. *J. Neurophysiol.* 36:409-424.
- Hoffmann, K.-P., and A. Schoppmann (1975) Retinal input to direction selective cells in the nucleus tractus opticus of the cat. *Brain Res.* 99:359-366.
- Illing, R.-B. (1980) Axonal bifurcation of cat retinal ganglion cells as demonstrated by retrograde double labelling with fluorescent dyes. *Neurosci. Lett.* 19:125-130.
- Illing, R.-B., and H. Wässle (1981) The retinal projection to the thalamus in the cat: A quantitative investigation and a comparison with the retinotectal pathway. *J. Comp. Neurol.* 202:265-285.
- Jhaveri, S., G.E. Schneider, and R.S. Erzurumlu (1991) Axonal plasticity in the context of development. In J.R. Cronly-Dillon (ed): *Vision and Visual Dysfunction*. Vol. XI: Development and Plasticity of the Visual System. London: MacMillan Press.
- Kelly, J.P., and C.D. Gilbert (1975) The projections of different morphological types of ganglion cells in the cat retina. *J. Comp. Neurol.* 163:65-80.
- Lehmkuhle, S., K.E. Kratz, S.C. Mange, and S.M. Sherman (1980) Spatial and temporal sensitivity of X- and Y-cells in the dorsal lateral geniculate nucleus of the cat. *J. Neurophysiol.* 43:520-541.
- Leventhal, A.G. (1982) Morphology and distribution of retinal ganglion cells projecting to different layers of the dorsal lateral geniculate nucleus in normal and siamese cats. *J. Neurosci.* 2:1024-1042.
- Leventhal, A.G., R.W. Rodieck, and B. Dreher (1985) Central projections of cat retinal ganglion cells. *J. Comp. Neurol.* 237:216-226.
- Linden, D.C., R.W. Guillery, and J. Cucchiaro (1981) The dorsal lateral geniculate nucleus of the normal ferret and its postnatal development. *J. Comp. Neurol.* 203:189-211.
- Linden, R., and C.A. Serfaty (1985) Evidence for differential effects of terminal and dendritic competition upon developmental neuronal death in the retina. *Neuroscience* 15:853-868.

- Majorossey, K., and A. Kiss (1976) Specific patterns of neuron arrangement and of synaptic articulation in the medial geniculate body. *Exp. Brain Res.* 26:1-17.
- Mesulam, M.-M. (1978) Tetramethyl benzidine for horseradish peroxidase neurohistochemistry: A non-carcinogenic blue reaction product with superior sensitivity for visualizing neural afferents and efferents. *J. Histochem. Cytochem.* 26:106-117.
- Mize, R.R., R.F. Spencer, and L.H. Horner (1986) Quantitative comparison of retinal synapses in the dorsal and ventral (parvicellular) C laminae of the cat dorsal lateral geniculate nucleus. *J. Comp. Neurol.* 248:57-73.
- Morest, K. (1965) The laminar structure of the medial geniculate body of the cat. *J. Anat. Lond.* 99:143-160.
- Morest, K. (1975) Synaptic relationships of Golgi type II cells in the medial geniculate body of the cat. *J. Comp. Neurol.* 162:157-194.
- Morgan, J.E., Z. Henderson, and I.D. Thompson (1987) Retinal decussation patterns in pigmented and albino ferrets. *Neuroscience* 20:519-535.
- Murphy, E.H., and R.E. Kalil (1979) Functional organization of lateral geniculate cells following removal of visual cortex in the newborn kitten. *Science* 206:713-716.
- Pallas, S.L., J.O. Hahm, and M. Sur (1989) Retinal axon arbors in a novel target: Morphology of ganglion cell axons induced to arborize in the medial geniculate nucleus of ferrets. *Soc. Neurosci. Abstr.* 15:495.
- Pallas, S.L., A.W. Roe, and M. Sur (1990) Visual projections induced into the auditory pathway of ferrets. I. Novel inputs to primary auditory cortex (A1) from the LP/pulvinar complex and the topography of the MGN-A1 projection. *J. Comp. Neurol.* 298:50-68.
- Pallas, S.L., J. Hahm, and M. Sur (1991) Axonal arborizations in the medial geniculate nucleus of ferrets: Comparison of arbors from the inferior colliculus with induced inputs from retinal ganglion cells. *Soc. Neurosci. Abstr.* 17:304.
- Payne, B.R., H.E. Pearson, and P. Cornwell (1984) Transneuronal degeneration of beta retinal ganglion cells in the cat. *Proc. R. Soc. Lond. [Biol.]* 222:15-32.
- Penny, G.R., D. Fitzpatrick, D.E. Schmechel, and I.T. Diamond (1983) Glutamic acid decarboxylase-immunoreactive neurons and horseradish peroxidase-labeled projection neurons in the ventral posterior nucleus of the cat and *Galago senegalensis*. *J. Neurosci.* 3:1868-1887.
- Perry, V.H., and A. Cowey (1982) A sensitive period for ganglion cell degeneration and the formation of aberrant retino-fugal connections following tectal lesions in rats. *Neuroscience* 7:583-594.
- Price, D.J., and J.E. Morgan (1987) Spatial properties of neurones in the lateral geniculate nucleus of the pigmented ferret. *Exp. Brain Res.* 68:28-36.
- Rodieck, R.W. (1979) Visual pathways. *Annu. Rev. Neurosci.* 2:193-225.
- Rodieck, R.W., and R.K. Brening (1983) Retinal ganglion cells: Properties, types, genera, pathway, and trans-species comparisons. *Brain Behav. Evol.* 23:121-164.
- Roe, A.W. (1991) Functional transformations of visual input by auditory thalamus and cortex: An experimentally induced visual pathway in ferrets. Doctoral dissertation, M.I.T., Cambridge, MA.
- Roe, A.W., P.E. Garraghty, and M. Sur (1989) The terminal arbors of single on-center and off-center X and Y retinogeniculate axons within the ferret's lateral geniculate nucleus. *J. Comp. Neurol.* 288:208-242.
- Roe, A.W., S.L. Pallas, J.O. Hahm, and M. Sur (1990) A map of visual space induced into primary auditory cortex. *Science* 250:818-820.
- Roe, A.W., J. Hahm, and M. Sur (1991) Experimentally induced establishment of visual topography in auditory thalamus. *Soc. Neurosci. Abstr.* 17:898.
- Roe, A.W., S.L. Pallas, Y.H. Kwon, and M. Sur (1992) Visual projections routed to the auditory pathway in ferrets: Receptive fields of visual neurons in primary auditory cortex. *J. Neurosci.* 12:3651-3664.
- Rowe, M.H. (1990) Evidence for degeneration of retinal W cells following early visual cortical removal in cats. *Brain Behav. Evol.* 35:253-267.
- Rowe, M.H., and B. Dreher (1982) Retinal W-cell projections to the medial interlaminar nucleus in the cat: Implications for ganglion cell classification. *J. Comp. Neurol.* 204:117-133.
- Schneider, G.E. (1973) Early lesions of superior colliculus: Factors affecting the formation of abnormal retinal projections. *Brain Behav. Evol.* 8:73-109.
- Sherman, S.M., and P.D. Spear (1982) Organization of visual pathways in normal and visually deprived cats. *Physiol. Rev.* 62:738-855.
- So, Y.-T., and R. Shapley (1981) Spatial tuning of cells in and around lateral geniculate nucleus of the cat: X and Y relay cells and perigeniculate interneurons. *J. Neurophysiol.* 45:107-120.
- Spear, P.D., D.C. Smith, and L.L. Williams (1977) Visual receptive field properties of single neurons in cat's ventral lateral geniculate nucleus. *J. Neurophysiol.* 40:390-409.
- Spreafico, R., D.E. Schmechel, L.C. Ellis, and A. Rustioni (1983) Cortical relay neurons and interneurons in the n. ventralis posterolateralis of cats: A horseradish peroxidase, electron microscopic, Golgi and immunocytochemical study. *Neuroscience* 9:491-509.
- Stanford, L.R. (1987a) W-cells in the cat retina: Correlated morphological and physiological evidence for two distinct classes. *J. Neurophysiol.* 57:218-244.
- Stanford, L.R. (1987b) X-cells in the cat retina: Relationships between the morphology and physiology of a class of cat retinal ganglion cells. *J. Neurophysiol.* 58:940-964.
- Stanford, L.R., and S.M. Sherman (1984) Structure/function relationships of retinal ganglion cells in the cat. *Brain Res.* 297:381-386.
- Stone, J. (1978) The number and distribution of ganglion cells in the cat's retina. *J. Comp. Neurol.* 180:753-772.
- Stone, J., and R. Clarke (1980) Correlation between soma size and dendritic morphology in cat retinal ganglion cells: Evidence of further variation in the g-cell class. *J. Comp. Neurol.* 192:211-217.
- Sur, M. (1988) Development and plasticity of retinal X and Y axon terminations in the cat's lateral geniculate nucleus. *Brain Behav. Evol.* 31:243-251.
- Sur, M., and S.M. Sherman (1982) Linear and nonlinear W-cells in C-laminae of the cat's lateral geniculate nucleus. *J. Neurophysiol.* 47:869-884.
- Sur, M., R.E. Weller, S.M. Sherman (1984) Development of X- and Y-cell retinogeniculate terminations in kittens. *Nature* 310:246-249.
- Sur, M., A.W. Roe, and P.E. Garraghty (1987b) Evidence for early specificity of the retinogeniculate X cell pathway. *Soc. Neurosci. Abstr.* 13:590.
- Sur, M., P.E. Garraghty, and A.W. Roe (1988) Experimentally induced projections into auditory thalamus and cortex. *Science* 242:1437-1441.
- Tong, L., and P.D. Spear (1982) Loss of retinal X-cells in cats with neonatal or adult visual cortex damage. *Science* 217:72-75.
- Vitek, D.J., J.D. Schall, and A.G. Leventhal (1985) Morphology, central projections, and dendritic field orientation of retinal ganglion cells in the ferret. *J. Comp. Neurol.* 241:1-11.
- Walsh, C., E.H. Polley, T.L. Hickey, and R.W. Guillery (1983) Generation of cat retinal ganglion cells in relation to central pathways. *Nature* 302:611-614.
- Wässle, H., and R.B. Illing (1980) The retinal projection to the superior colliculus in the cat: A quantitative study with HRP. *J. Comp. Neurol.* 190:333-356.
- Williams, R.W., and L.M. Chalupa (1982) Prenatal development of retinocollicular projections in the cat: An anterograde tracer transport study. *J. Neurosci.* 2:604-622.
- Wilson, J.R., M.J. Friedlander, and S.M. Sherman (1984) Fine structural morphology of identified X- and Y-cells in the cat's lateral geniculate nucleus. *Proc. R. Soc. Lond. [Biol.]* 221:411-436.
- Wilson, P.D., M.H. Rowe, and J. Stone (1976) Properties of relay cells in cat's lateral geniculate nucleus: A comparison of W-cells with X- and Y-cells. *J. Neurophysiol.* 39:1193-1209.
- Wingate, R.J.T., T. Fitzgibbon, E.I. Webb, and I.D. Thompson (1990) Lucifer yellow, fluorescent retrograde tracers and fractal analysis characterize ferret retinal ganglion cells. *Soc. Neurosci. Abstr.* 16:1216.
- Zahs, K.R., and M.P. Stryker (1985) The projection of the visual field onto the lateral geniculate nucleus of the ferret. *J. Comp. Neurol.* 241:210-224.